A Review of Spatial Markov Models for predicting pre-asymptotic and anomalous transport in porous and fractured media

Thomas Sherman[a], Nicholas B. Engdahl[b], Giovanni Porta[c], Diogo Bolster[a]

[a] *Civil and Environmental Engineering and Earth Sciences, University of Notre Dame, South Bend, IN, USA*
[b] *Department of Civil and Environmental Engineering, Washington State University, Pullman, WA, USA*
[c] *Dipartimento di Ingegneria Civile ed Ambientale, Politecnico di Milano, Piazza L. Da Vinci, 32, 20133 Milano, Italy*

Abstract

Heterogeneity across a broad range of scales in geologic porous media often manifests in observations of non-Fickian or anomalous transport. While traditional anomalous transport models can successfully make predictions in certain geological systems, increasing evidence suggests that assumptions relating to independent and identically distributed increments constrain where and when they can be reliably applied. A relatively novel model, the Spatial Markov model (SMM), relaxes the assumption of independence. The SMM belongs to the family of correlated continuous time random walks and has shown promise across a wide range of transport problems relevant to natural porous media. It has been successfully used to model conservative as well as more recently reactive transport in highly complex flows ranging from pore scales to much larger scales of interest in geology and subsurface hydrology. In this review paper we summarize its original development and provide a comprehensive review of its advances and applications as well as lay out a

vision for its future development.

1. Introduction

Heterogeneity is a characteristic feature of natural porous media and the complex geological media that make up the subsurface, and their associated flow and transport processes, span a vast range of scales from nanometers to hundreds of kilometers (1). Subsurface heterogeneities occur at every scale and specific forms include physical heterogeneities like transitions between hydrofacies (2), chemical heterogeneities that reflect changing mineralogies (3), and biological heterogeneities like biofilm growth (4), among others. Each kind of heterogeneity can strongly influence the velocity at which substances can move through the porous medium or their residence times. One of the most influential parameters on transport is certainly the intrinsic permeability of the medium, which governs fluid velocity and pressure through Darcy's law. Permeability is linked to hydraulic conductivity and can vary by orders of magnitude over relatively short distances. This extreme variability often yields behaviors that exhibit broad spatial and temporal velocity distributions, which are not predicted well by classical, continuum-based transport theories that model linear scaling of the mean squared displacement, i.e. by specifying Fickian dispersion with constant coefficients. The transport of contaminants, nutrients, other dissolved substances, such as bacteria, colloids, nanoparticles, viruses, etc. often exhibits nonlinear temporal scaling of the mean squared displacement ($\langle x^2 \rangle \sim t^\alpha; \alpha \neq 1$) over time scales of practical interest (5; 6), and thus is classified as displaying "anomalous" transport characteristics; superdiffusive transport is obtained for $\alpha > 1$ with

subdiffusive transport occurring in the opposite case. Since transport in natural porous media routinely violates the assumptions of the prevailing state-of-the-art models, we need models that can capture the influence of heterogeneity across this range of scales that causes these deviations.

Much of the early work on developing effective transport models in porous media built on the pioneering ideas of Taylor (7) and Aris (8). These seminal works demonstrated that transport can be described by an effective advection-dispersion equation with a Fickian dispersion coefficient when a plume is given sufficient time to sample the full distribution of heterogeneous velocity scales. Common approaches following this idea include the method of moments (9), volume averaging (10) and homogenization (11; 12). As powerful and elegant as these upscaling approaches are, they are restricted in their application for three main reasons: i) they are limited to specific ranges of transport regimes, e.g., in terms of Péclet or Damköhler numbers (the latter in the case of reactive transport), ii) they require the definition of a spatially periodic unit cell to compute effective parameters and iii) the effective coefficients so derived may be valid only at asymptotic times, which may be prohibitively long depending on the underlying flow structure. Other pioneering works studying dispersion in porous media include (13) and (14), who introduced the concept of residence times to study particle displacement statistics.

In general, anomalous transport behaviors can be predicted, starting from a detailed model of the system heterogeneity. This, for example can be obtained by applying an effective Fickian transport model at local scales where the heterogeneity of the system is fully resolved, as it is in a multi-

dimensional, spatially distributed model of flow and transport (15; 16; 17; 18; 19). Once a spatial resolution is chosen to represent heterogeneity, this effectively averages out the sub-grid heterogeneity, allowing transport in each cell to be modeled as a Fickian process, but the interactions between cells with disparate velocities lead to larger scale non-Fickian behaviors (20; 21; 22; 23; 24). The main issue with this approach is that it requires a detailed model of the subsurface heterogeneities; the inaccessibility of the subsurface means that geostatistical techniques are required to approximate it (25; 26). In fully saturated media (e.g., at aquifer scale) perturbation approaches may be used to characterize transport statistics as a function of a permeability spatial heterogeneity model (e.g. 27). However, these linearized approaches become inaccurate for increasing degrees of heterogeneity (i.e. when the variance of natural logarithm of hydraulic conductivity exceeds unity). Even beyond the mere estimation of the intrinsic permeability, significant uncertainty exists in the parameter fields (e.g., porosity) as well as the initial and boundary conditions, and this may require numerically evaluating ensemble statistics to quantify the uncertainty, all of which is computationally expensive. Similar issues arise when considering non-Fickian behavior emerging from pore scale simulations (28; 29): anomalous transport can be predicted using a pore scale model, but this is computationally unfeasible in real, large-scale applications, i.e. beyond mm-scale samples. In short, the uncertainty and complexity of a distributed parameter model may outweigh its benefits in a predictive capacity and this further motivates the need for simplified, or upscaled, models.

A variety of upscaled models have been proposed to describe anomalous

transport in geological porous media and have been applied with success. Some of the most widely used are multi-rate mass transfer (MRMT) (30), fractional advection dispersion models (fADE) (31) and continuous time random walks (CTRW) (32). It is important to emphasize that these are by no means the only anomalous transport models used in porous media, but the most widely used, due to their demonstrated success across a wide range of temporal and spatial scales. Their dissemination into the scientific community has been also promoted by openly available computational toolboxes (33; 34; 35). Despite the specifics of their individual origins, it is noteworthy that these models are all highly inter-related (e.g. 36; 37; 38; 39; 40). Choosing any one model over another typically depends on the conceptual model developed by the user, which often aligns more naturally with one framework than the others. It has been shown that all of these models can be represented by a random walk or by Eulerian nonlocal (integro-differential) partial differential equations. We focus in this review on Lagrangian approaches where particles transition through space and time following prescribed rules (41; 32; 31). Random walks in general are commonly used in the study of transport in porous media as highlighted in a review by Noetinger et al (42). Classical Fickian transport can be represented as a random walk, but the primary difference is that anomalous transport is generated when the distributions of random increments (in space or time) have infinite variance or mean (43). As such, the broad or heavy tailed distributions cannot converge by the central limit theorem to classical Fickian limiting behavior, resulting in anomalous transport.

It is important to note that, in most implementations of Lagrangian ran-

dom walk models (Fickian or non-Fickian), successive increments are either implicitly or explicitly assumed to be independent and identically distributed. While this is a common assumption, it is not necessarily correct. In this context, Le Borgne and co-workers (44) clearly showed the importance of correlation for geologically realistic heterogeneous porous media and suggested a need to develop models that relax the assumption of independence. Other authors (Painter and Cvetkovic) (45; 46; 47), studying transport in fractured geologic media, also demonstrated the existence and importance of correlation effects that must be included to upscale transport correctly. This can be achieved upon modeling transport by considering probabilistic rules to determine residence times in successive steps using a Markov chain, as was already envisaged in earlier works (13). In a conceptual sense, consider that it is more likely for rapidly moving solute particles to continue moving quickly over small time scales than they are to abruptly slow down; the latter is possible but less likely on average, thus violating the assumption of independent transitions. For practical problems relating to transport through porous media, the spatial scale where transitions become independent may be larger than the scales of interest for predictions. Later numerical studies of flow through highly heterogeneous porous media by Le Borgne *et al.* (20; 48) showed similar behavior, including a dependence of Lagrangian correlations on the local velocity as well as the ability for a particle to experience abrupt changes in velocities. From these observations, they suggested and then verified that velocities at equidistant positions along a particle trajectory form a Markov process. In particular, they confirmed that fast particles tended to persist at being fast and slow particles tended to remain slow at fixed spatial

increments. From this, they justified a fixed spatial step Langevin equation where successive increments in time are correlated (reflecting velocity correlation between individual particles' steps); this kind of model is what we call the Spatial Markov Model (SMM). The SMM has shown great promise in replicating simulated and observed transport behaviors across the diverse range of settings and transport scales in geological porous media. The model has also gone by the name correlated CTRW and we will use the names interchangeably throughout this article, although it should be noted that the name correlated CTRW pertains to a broader family of models than just the SMM.

The objective of this article is to provide an overview of the SMM and its many developments and applications over the last decade or so. We open with a general overview of the method in Section 2 followed by its historical development, and applications in porous and fractured media at multiple scales. A discussion of random walks defined in terms of analytical models of velocity transitions is then provided, complemented with an overview of SMM applications to nonlinear transport processes. We then close with a critical review of the challenges, limitations, and avenues for improving the model in the future and consider how to improve parameterizations and parameter identification, as well as how to link specific SMM model elements with the properties of natural geological media. The work presented here focuses exclusively on the development and application of such models in the context of geologic media; however, it must be noted that correlated CTRWs, similar in nature to the SMM presented here, play an important role in other branches of physics also (49; 50). As noted by Magdziarz *et al.* (51), cor-

relations arise when dealing with living systems, including bacterial motion (52), the ecology of animal motion (53) and human mobility (54), as well as in other dynamic systems such as financial markets (55; 56), seismology (57) and chaotic and turbulent flows (58).

2. The Spatial Markov Model

The SMM is a particle based random walk model that simulates transport. The system is described by a large number of particles N, where during each step a particle takes a uniform fixed step in space of size L $[L]$. In this sense it can be seen as a CTRW model, or as a time domain random walk model (TDRW), using the distinction noted by Aquino & Dentz (59). The amount of time it takes to perform the step is random, but, unlike other approaches, it is not independent and is conditioned on the time taken to execute the previous step. We then describe transport of each particle according to the discrete equation

$$\begin{aligned} x^{(n+1)} &= x^{(n)} + L \\ t^{(n+1)} &= t^{(n)} + \tau^{(n+1)} \quad n = 0,1,2,... \end{aligned} \tag{1}$$

where $x^{(n)}[L]$ is the particle position at step n, $t^{(n)}$ $[T]$ denotes the total travel time at step n and the transition time, $\tau^{(n+1)}$ $[T]$, is sampled from

$$f(\tau) = \begin{cases} f(\tau_1) & \text{if } n{=}\ 0 \\ f(\tau^{(n+1)}|\tau^{(n)}) & \text{if } n = 1,2,\ldots . \end{cases} \tag{2}$$

where $f[-]$ is a joint distribution function of transition times between the discrete travel times. In practice, SMM applications have predominately been

167 1-d, which significantly reduces the complexity and data requirements of the
168 upscaled model, but multi-dimensional forms also exist (e.g. 60; 61; 62).

The distribution of transition times, $f(\tau_1)$, is defined as part of the parameterization of a specific SMM and $f(\tau_2|\tau_1)$ is modeled using a conditional transition matrix. To obtain the transition matrix, $f(\tau_1)$ is separated into N discrete bins (typically, but not necessarily, equiprobable), where N is sufficiently large for convergence (63). Bin 1 contains the particles with the fastest travel times and Bin N contains particles with the slowest travel times. A particle with travel time τ_p is in Bin i if $t_{c,i} \leq \tau_p < t_{c,i+1}$, where $t_{c,i}$ is the cutoff time for Bin i, $t_{c,1} = 0$, and $t_{c,N+1}$ is greater than the maximum value of τ_1 and τ_2 for all particles. Then, the transition matrix is defined by

$$T_{i,j} = P(\tau_2 \in \text{Bin } j | \tau_1 \in \text{Bin } i) \approx f(\tau_2|\tau_1). \tag{3}$$

169 It is assumed that the process is stationary such that $f(\tau^{(n+1)}|\tau^{(n)}) = f(\tau_2|\tau_1)$.
170 Thus, each block of the transition matrix, $T_{i,j}$, describes the probability that
171 a particle will have a travel time in Bin j given that its travel time was in
172 Bin i in the previous step. A typical transition matrix, in this case taken
173 from a pore scale flow by Le Borgne *et al.* (63), is shown in Figure 1.

174 For equiprobable binning of the travel time distribution, an uncorrelated
175 CTRW can be obtained in this formulation if $T_{i,j} = 1/N \ \forall \ i, j$. This creates
176 a uniformly distributed transition matrix where all bins are equally accessi-
177 ble to all others, meaning that the conditional probability $f(\tau^{(n+1)}|\tau^{(n)}) =$
178 $f(\tau_{n+1})$, and there can be no correlation between steps. Indeed, strictly
179 speaking an uncorrelated series of waiting times also represents a Markov
180 model, a so-called Markov-0 model. Thus, in this sense, any continuous time
181 random walk for the modeling of particle positions in space is based on a

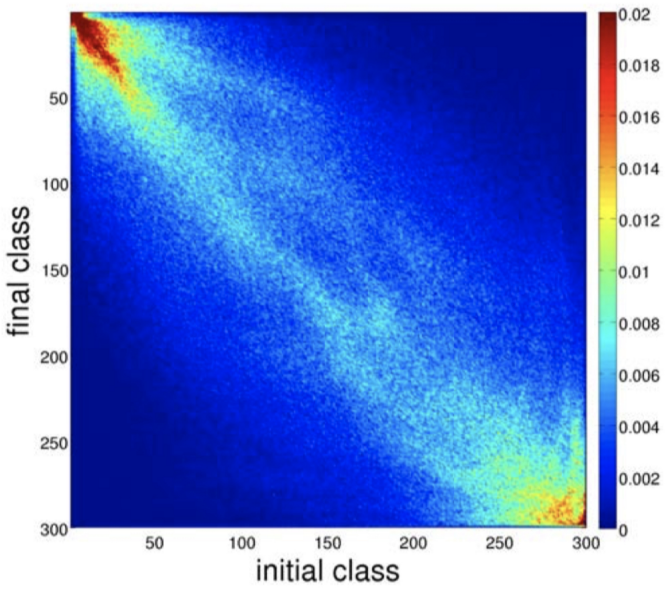

Figure 1: A typical spatial transition matrix for SMMs in porous media, where classes with low (high) numbers have associated fast (slow) transit times. Each transit travel time has a corresponding travel distance equal to the mean pore size. Adapted with permission from (63).

spatial Markov process. A non-uniform transition matrix is the distinguishing feature of the SMM as we refer to it here, relative to their uncorrelated CTRW cousins. The travel times, τ^n, for each step along the path is drawn from the conditional distributions, and this produces the total time to reach the nth step. Conceptually, the resulting paths share some similarity with stochastic-convective transport models (64; 65) or a streamtube ensemble (66; 67; 68).

3. Development, Applications and Implications

3.1. Transport in Highly Heterogeneous Permeability Fields

The first application of the SMM in the context of porous media flows was performed by Le Borgne *et al.* (20; 48), who were interested in upscaling transport of a conservative scalar through highly heterogeneous porous media represented by a Darcy continuum. Darcy-type flow is described by

$$\mathbf{q}(\mathbf{x}) = -\mathbf{K}(\mathbf{x})\nabla h \tag{4}$$

where $\mathbf{K}$ $(\mathbf{x})[L/T]$ is a hydraulic conductivity tensor, h $[L]$ is the head (potential), and the so-called Darcy velocity is $\mathbf{q}(\mathbf{x})$ $[L/T]$. The Darcy velocity is a mass averaged velocity resulting from the homogenization of pore scale flows that are not explicitly represented in the upscaled model, so the influence of all processes below the support scale of the Darcy continuum are embedded in the effective parameter $\mathbf{K}(\mathbf{x})$, which is often reduced to a single scalar value K, assuming an isotropic medium, which is questionable in geologic media but often invoked for simplicity. Given the size of geologic systems, it is typically not feasible, not possible and not even desirable, to represent pore

scales in their full detail for domains larger than a soil column (i.e. beyond the characteristic length scale of cm-dm). As such, an effective continuum perspective is typically considered when studying practical applications of transport in geologic systems, i.e. velocity is approximated through Darcy's law. The Darcy velocity is defined to maintain continuity of the flow and is not the mean pore-water velocity $\mathbf{v}(\mathbf{x})[L]$, that dictates how solutes advect, but this can be obtained from $\mathbf{v}(\mathbf{x}) = \mathbf{q}(\mathbf{x})/\phi(\mathbf{x})$ where $\phi[-]$ is the porosity.

One of the challenges in groundwater hydrology is developing accurate transport models for highly heterogeneous systems, for which the variance of the log conductivity field is typically much larger than one ($\sigma^2_{lnK} > 1$). While it is known that the limit $\sigma^2_{lnK} < 1$ may be respected within individual geological depositional units (69; 70), the hierarchical nature of large-scale geological formations juxtaposes geomaterials with dramatically different K ranges over short distances and this causes σ^2_{lnK} to grow rapidly.

Le Borgne *et al.* investigated 2-d hydraulic conductivity fields that were well above the $\sigma^2_{lnK} > 1$ threshold. In particular, they studied transport in three heterogeneous systems, that contain several of the important features of real geologic systems: (i) a multilognormal K field, (ii) a field with identical variance but fully connected highly permeable preferential flow paths, and (iii) a stratified system with $\sigma^2_{lnK} = 9$. The K fields were characterized by an isotropic correlation distance λ. Sample conductivity and associated velocity fields are shown in Figure 2. All three fields have identical point distributions of hydraulic conductivity values, but clearly vary in their structure and this creates velocity fields that vary by over 10 orders of magnitude. The velocity fields also exhibit varying degrees of connectivity in terms of slow regions

and longer connected fast flow channels as one moves from (i)-(iii). The more connected fields typically result in earlier first arrivals and larger late arrivals with more disperse breakthrough curves, reflecting that fast particles persist at being fast to arrive quickly and slow particles persist at being slow (trapped) to arrive later.

The fields shown in Figure 2 were used to develop a domain-wide, upscaled model of the longitudinal (mean flow direction) Lagrangian velocities defined as

$$v_L = \frac{x_{n+1} - x_n}{t(x_{n+1}) - t(x_n)} \tag{5}$$

which accounts for diffusive and advective motion. The velocities were defined by considering the probability for a particle to transition from velocity v' at travel time t' to velocity v at travel time t

$$r_t(v, t|v', t') = \langle \overline{\delta(v - v_t(t))} \rangle_{v_t(t')=v'} \tag{6}$$

as well as the probability for a particle to make a transition from velocity v' at travel distance x' to velocity v at travel distance x

$$r_s(v, x|v', x') = \langle \overline{\delta(v - v_s(x))} \rangle_{v_s(x')=v'}. \tag{7}$$

After discretizing the velocity distribution into N equiprobable classes, they defined the temporal and spatial velocity transition matrices for temporal increment t and the spatial increment s as

$$T^t_{i,j} = \int_{v_i}^{v_{i+1}} \int_{v_j}^{v_{j+1}} r_t(v,t|v',t')dv'dv \qquad T^s_{i,j} = \int_{v_i}^{v_{i+1}} \int_{v_j}^{v_{j+1}} r_s(v,x|v',x')dv'dv \tag{8}$$

where $T_{i,j}$ is the probability to make a transition from a velocity $v' \in C_j$ to a velocity $v \in C_i$.

These metrics allowed Le Borgne *et al.* to demonstrate that the Lagrangian velocity fields are characterized by a broad range of correlation times, as quantified by T^t, but a relatively narrow range of correlation distances, as quantified by T^s. Based on this observation the authors applied a test for Markovian behavior in space and time. In order to describe a Markov chain, the Chapman-Kolmogorov condition requires that the transition matrix must satisfy

$$\mathbf{T}(\omega + \omega') = \mathbf{T}(\omega)\mathbf{T}(\omega') \qquad \Rightarrow \qquad T(n\omega) = T^n(\omega), \tag{9}$$

where ω is a dummy variable. The analysis revealed that Markovian behavior in time was never observed over the time scales considered, owing to a broad distribution of correlation times, but that spatial increments greater than $\lambda/2$ were Markovian. These observations motivate the use of an SMM as described in § 2 and also explain the origin of the name.

The SMM model was proposed by Le Borgne *et al.* (48) and applied in (20) to predict two commonly measured features in porous media: (i) first passage time distributions at a distance 12.5λ corresponding to a flux weighted initial line condition spanning most of the vertical extent of the domain and (ii) evolution of the spatial variance of the concentration field. In both cases, the results of a fully resolved direct numerical simulation (DNS)

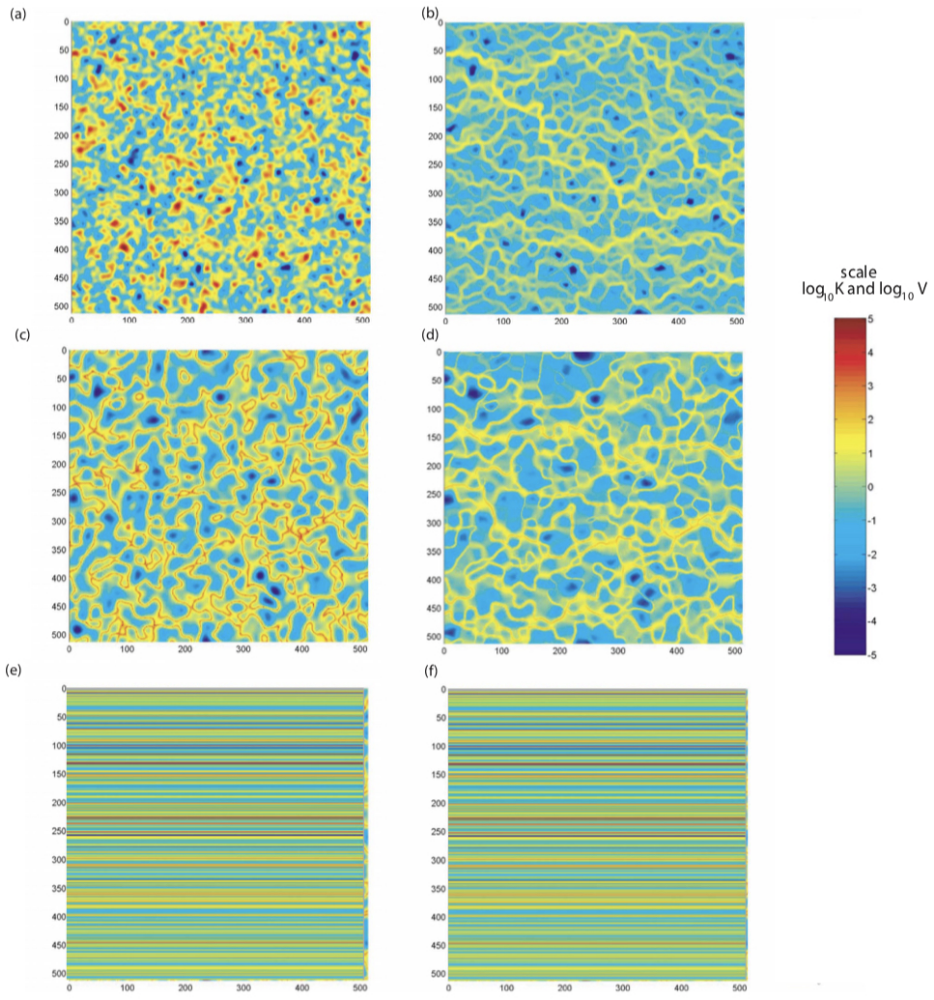

Figure 2: The hydraulic connectivity K (left) and corresponding velocity fields (right) studied by Le Borgne *et al.* (48). All three fields have the same point K distribution. Row 1 is a multilognormal connectivity field with $\sigma_f^2 = 9$; row 2, a connected hydraulic connectivity field; and row 3, a stratified hydraulic connectivity field. Adapted with permission from (48)

were compared to predictions made with an SMM, as well as a model that considers no correlation between successive spatial steps (referred to in their paper a classical CTRW, although we will not adopt that notation here). Their results are shown in Figure 3 and demonstrate that the SMM can reproduce the dominant features of the DNS, whilst the model that does not account for correlation is unable to accurately reproduce the DNS. Most notably, the uncorrelated model fails to adequately capture early arrivals, but it also under-predicts late time arrivals for the multi-lognormal case, which can be summarized as under-estimating spreading over time. The example clearly demonstrates the importance of accounting for velocity correlation since both models (correlated and uncorrelated) used the same limited information in the space-time domain of interest to infer velocity distributions at larger scales. The concept is simple enough in principle, whereby fast particles tend to persist at being fast (i.e. once in a fast channel they can remain their for quite a while) and slow particles can also persist at being slow, but it has a profound impact on the performance of the upscaled transport model. It should be noted that the same numerical dataset was later analyzed by (71) with an uncorrelated CTRW, which was also able to accurately reproduce the DNS data. This can be explained by observing that the correlated model will ultimately converge to an uncorrelated one (72), whose space-time transitions pdf is of course different than the one measured on a smaller scale.

3.2. Transport in Fractured Media

Another common setting that is of interest in the geosciences is flow through fractured media, where flow, rather than occurring through pore

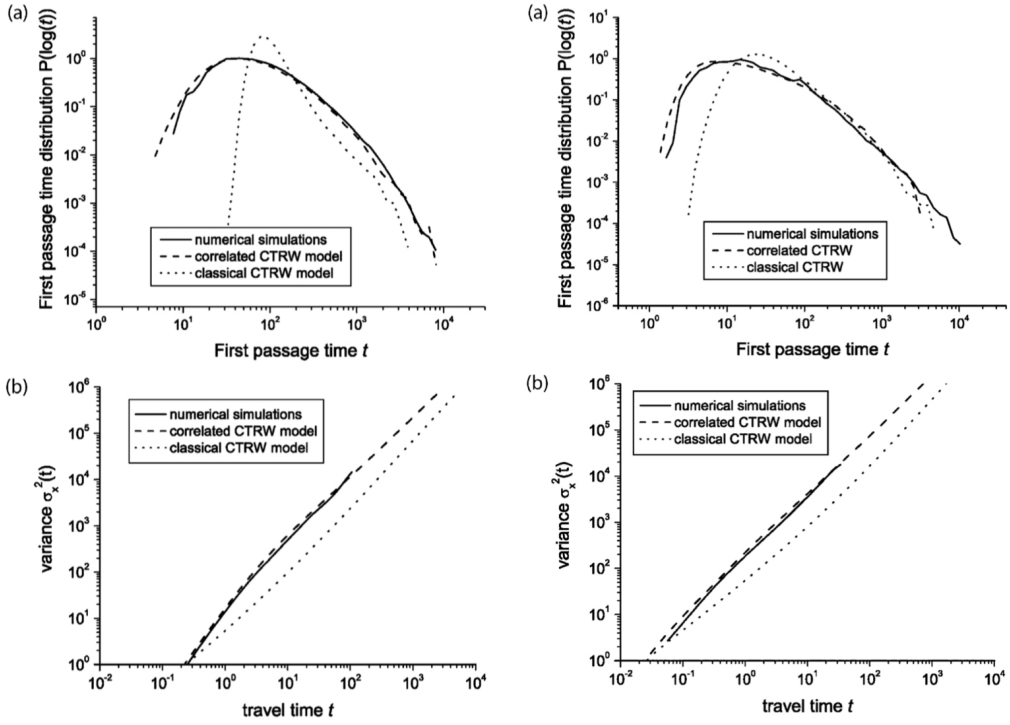

Figure 3: First passage time distributions and temporal evolution of the plume variance for multilognormal and connected hydraulic connectivity fields. Numerical simulations are compared with correlated and uncorrelated CTRW models. Adapted with permission from (20)

spaces in unconsolidated media, happens through fractures in an otherwise near impermeable rock matrix. Such settings are common in nature and the broad range of fracture properties and architectures are known to result in complex flow networks that display anomalous transport (e.g. 73). Anomalous transport in such systems may arise from different physical characteristics that define the fractures, such as the aperture of individual fractures or the angle between the fracture direction and the average pressure gradient. The spatial arrangement of fracture intersections also plays a relevant role in this context. Painter, Cvetkovic and coauthors, using discrete fracture network models to simulate flow and transport in fractured geologic media, demonstrated the existence and importance of correlation effects that must be included to upscale transport correctly (45; 46; 47).

In the context of the SMM, Kang *et al.* (60) studied flow and transport in a fractured medium. To focus only on one form of heterogeneity, they idealized their fracture network, as depicted in Figure 4. Their lattice is made up of two sets of parallel, equidistant links separated by distance l. The links are oriented at a fixed angle α with respect to the longitudinal x axis. The flow is driven by a unit potential drop in the longitudinal direction ($\Phi = 1$ at the inlet and $\Phi = 0$ at the outlet). Along each link flow is governed by Darcy type flow (an averaged Poiseuille flow) where the flow velocity depends on the fracture conductivity (k), length (l) and potential drop across a fracture such that for a link between node i and j the velocity is $u_{ij} = k_{ij}\frac{\Phi_i - \Phi_j}{l}$. A further physical constraint of incompressibility is imposed such that the sum of all inflows and outflows at a node is zero; i.e. at node i $\sum_j u_{ij} = 0$. This results in a linear set of equations that can readily be

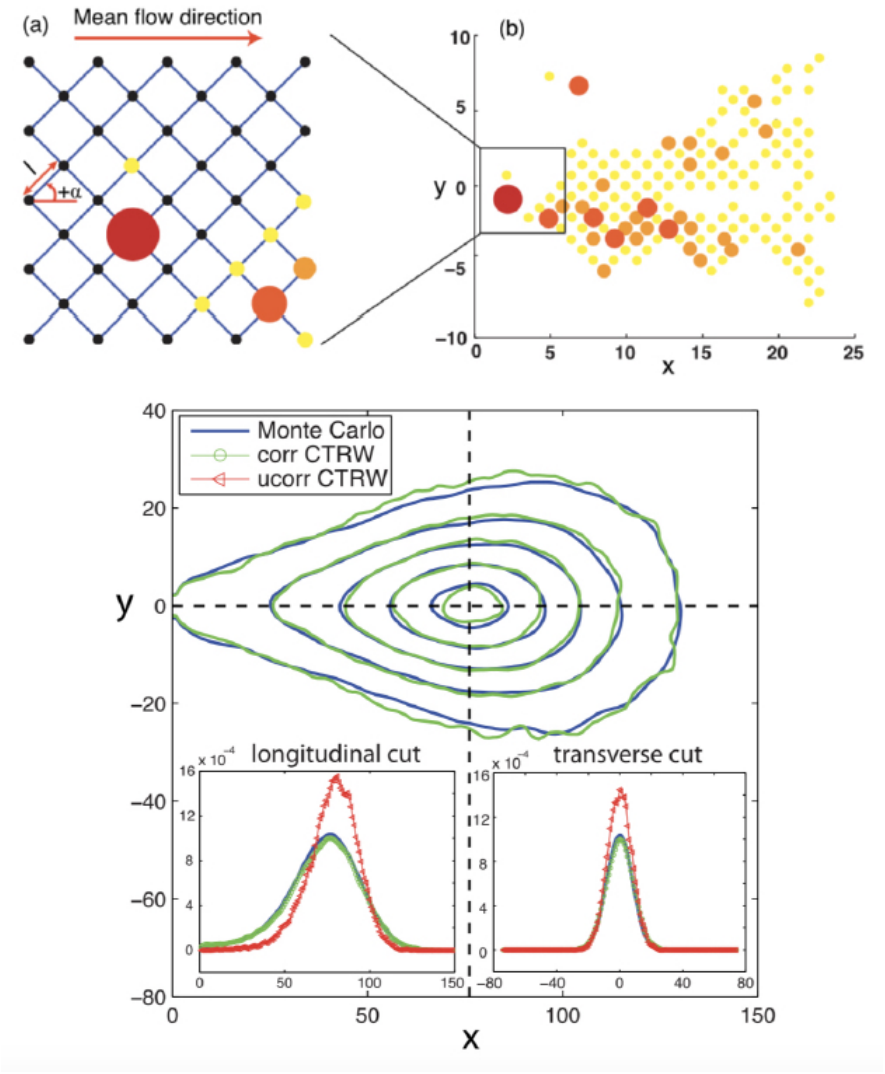

Figure 4: (Top) A schematic of the lattice networks considered by Kang *et al.* (60). Lattice link velocities are independent and identically distributed and network realizations are quenched disordered in particle velocities. A snapshot of particle density (circle size) for t=30, where particles initialize at $x = 0$ (b). (Bottom) A contour plot of ensemble averaged particle density at fixed time for the lattice networks considered by Kang *et al.* (60). Monte Carlo ensemble averaged particle densities are compared with predictions from an uncorrelated and correlated CTRW. Adapted with permission from (60)

solved. The only form of heterogeneity that the authors considered was in the fracture conductivities k, where each link was assigned an independent and identically distributed value (they considered lognormal, Cauchy and truncated power law distributions); that is there is no correlation imposed in the medium structure. From this setup, the set of all realizations of the random fracture network form a statistical ensemble that is both stationary and ergodic. They then perform particle tracking simulations, neglecting diffusion and assuming complete mixing at each node (i.e. a particle's exit from each node is determined randomly by flux- weighted probability). Considering a point initial condition $\mathbf{x}(t=0) = \delta(\mathbf{x})$, they run simulations over O(1000) realizations, and average over realizations to obtain mean particle density $P(\mathbf{x}, t)$.

As in (20), Kang *et al.* studied individual particle trajectories by considering ensemble statistics of Lagrangian velocities and focusing on transition times at fixed space increments as in (7). They demonstrated that correlation between subsequent transition times does indeed exist. Despite the fact that the random fracture permeabilities are completely independent, the imposition of incompressibility induces correlation in space, i.e. flow develops along minimum resistance pathways that connect inflow to outflow. They also successfully demonstrated that a Markov model predicted the transition probabilities, suggesting that a SMM may be a suitable upscaled model. They proposed such a correlated CTRW, where particle locations are governed by the following equation

$$\mathbf{x}_{n+1} = \mathbf{x}_n + l\frac{\mathbf{v}_n}{|\mathbf{v}_n|} \qquad t_{n+1} = t_n + \frac{l}{|\mathbf{v}_n|}. \tag{10}$$

Successive velocities follow a Markov chain with one step transition probability density as in 7. From this the particle density can be written as

$$P(\mathbf{x},t) = \int \int_{t-l/|\mathbf{v}|}^{t} R(\mathbf{x},\mathbf{v},t')dt'dv \qquad \text{where} \qquad R(\mathbf{x},\mathbf{v},t') = \langle \delta(\mathbf{x}-\mathbf{x}_n)\delta(\mathbf{v}-\mathbf{v}_n)\delta(t'-t_n)\rangle. \tag{11}$$

where $R(\mathbf{x},\mathbf{v},t')$ represents the particle distribution in space, velocity and time after n steps. It satisfies Kolmogorov type recursion equation

$$R(\mathbf{x},\mathbf{v},t') = \delta(\mathbf{x})p(\mathbf{v})\delta(t) + \int \int r(\mathbf{v}|\mathbf{v}')\delta(\mathbf{x}-\mathbf{x}'-l\mathbf{v}'/|\mathbf{v}'|)R(\mathbf{x}',\mathbf{v}',t')dx'dv', \tag{12}$$

which describes how this distribution evolves over successive jumps. If one assumes that successive jumps are uncorrelated, i.e. $r(v|v') = p(v)$, then an uncorrelated CTRW model is recovered, where

$$P(\mathbf{x},t) = \int_0^t \int_{t-t'}^{\infty} \int R(\mathbf{x},t')\psi(\mathbf{x},\tau)d\mathbf{x}d\tau dt' \tag{13}$$

with recursion equation

$$R(\mathbf{x},t') = \delta(\mathbf{x})\delta(t) + \int \int R(\mathbf{x}',t')\psi(\mathbf{x}-\mathbf{x}',t-t')dx'dt' \tag{14}$$

and joint transition length and time density is given by

$$\psi(\mathbf{x},t) = \int p(v')\delta(x - l\mathbf{v}'/|\mathbf{v}'|)\delta(t - l/|\mathbf{v}'|)d\mathbf{v}'. \tag{15}$$

Finally, Kang *et al.* compare the results from fully resolved DNS simulations to predictions obtained with both the correlated and uncorrelated

CTRW models. Their results are shown in Figure 4 (bottom). Particle density is non-Gaussian in space, having a sharp leading edge and elongated tail. As in (20), an uncorrelated model where subsequent transition times are random and mutually independent and are drawn from numerically measured distributions fails to accurately capture the full behavior of the system. Similar mismatches (not shown here) are observed in predictions of first passage times and evolution of second centered moments in time, which persist in displaying anomalous superdiffusive growth over the full range of space and times considered. It is worth repeating here that there is no correlation in the fracture network permeability field, but rather that this correlation structure emerges due to the fact that mass must be balanced at each node and the flow is incompressible. The application of this approach to a fractured rock field site (74) is described in further detail in §3.5. The model presented in this section has been further elaborated in (75; 76). Other recent applications in random discrete fracture networks of potential interest include (77; 78; 79; 80).

3.3. Transport at pore scales in porous media

Working at the continuum (Darcy) scale of flow and transport is practical when studying systems at geologic scales, as was the case in the previous two sections, but it is also important to recognize that heterogeneity in the flow exists below those scales, within individual pores and fractures. Most natural media are highly complex at this scale and the resulting flows can have a very broad range of transport time and velocity scales, leading to anomalous behaviors. While this complexity is often ignored and replaced with an effective advection-dispersion equation at Darcy scales, it is well

known that such an effective model rests on strong assumptions that are often not met and that can lead to incorrect predictions. Most of these effective models are built on ideas relating to Taylor dispersion (7), which is strictly only valid at asymptotic times; that is at a time $\tau_D > L^2/D$ where L is a characteristic length and D the diffusion coefficient. Physically this timescale represents the characteristic time it takes a particle to sample a system's full velocity variability. Depending on the system in question or the problem being solved, it may not be possible to reach the characteristic time scale so models capable of representing behaviors below this are needed.

3.3.1. Pore Scale SMMs

Le Borgne *et al.* in (63) were the first to apply the SMM in the context of a pore scale flow and transport setting. They considered a two dimensional porous medium as depicted in Fig 5. The medium is made up of voids and circular grains of two diameters that fill the space resulting in a porosity of 0.42. The flow is driven by a uniform pressure drop from top to bottom. Periodic conditions are imposed for flux on all boundaries. This particular domain was chosen as it had been the basis of previous transport upscaling studies (81; 82) due to the fact that the velocity field displays interesting features, including a braided network of preferential flow paths as well as low-velocity and stagnation zones, two features that are often associated with anomalous or highly non-Fickian pre-asymptotic transport. Dispersion in this setting has been observed to be superdiffusive (over 2 orders of magnitude in time), with higher-order moments further reinforcing that transport is strongly anomalous (83).

The authors compute the transit time and the transition matrix due to

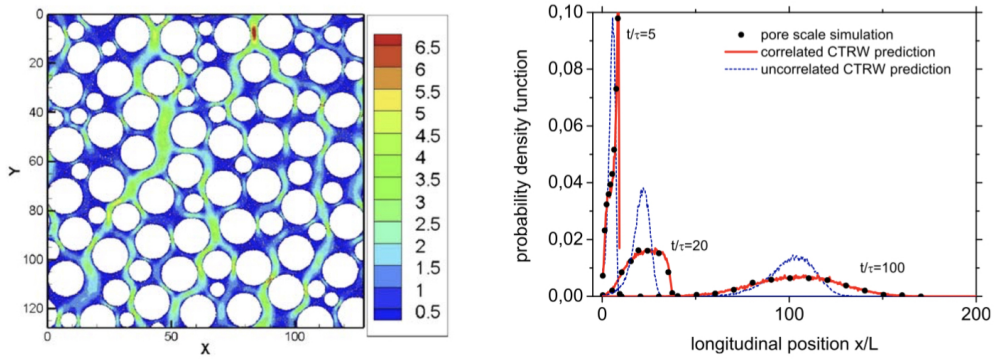

Figure 5: (Left) The pore scale geometry and velocity field used in (63). (Right) A comparison of the longitudinal distribution of particle positions between pore scale simulations, a correlated and an uncorrelated model. Adapted with permission from (63)

purely advective transport over a distance corresponding to the mean pore length. The resulting transition matrix is depicted in Figure 1 and, as with previous studies, depicts a strong diagonal dominance, reflecting that particles will most likely persist to move at a similar velocity with the two strongest hot spots at the extremes: fast particle persist at being fast (i.e. they are trapped in fast channels) and slow particle persist at being slow. A comparison of the distribution of longitudinal position of particles from a line injection at the boundary at various times between numerical results from high resolution direct numerical simulation as well as correlated and uncorrelated CTRW models is shown in Figure 5. The SMM is well able to reproduce the pore scale DNS values, even at the very earliest times, while the uncorrelated model fails.

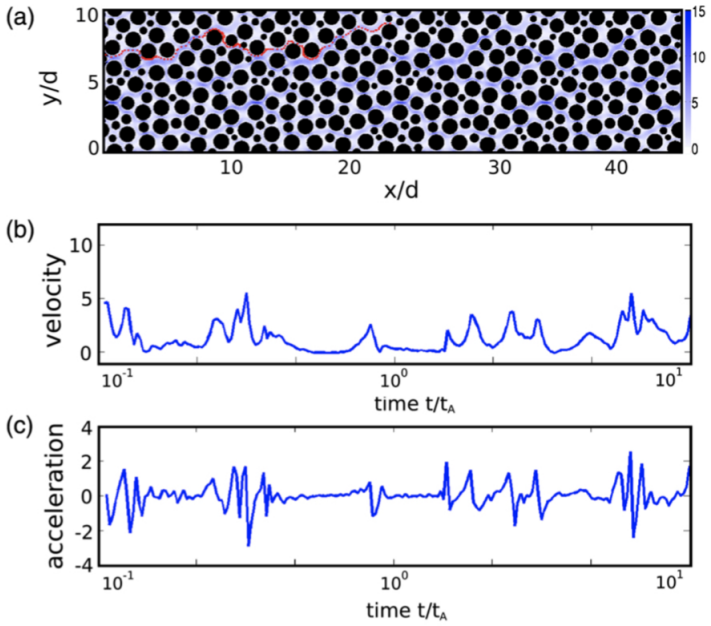

Figure 6: The pore scale velocity field for an idealized porous medium with a particle trajectory highlighted in red (a). (b) and (c) display particle velocity and acceleration through time. Notice the intermittent behavior of the particle trajectory, i.e. long periods of slow velocity and no acceleration followed by short periods of abrupt accelerations. Adapted with permission from (83)

3.3.2. Intermittency

The results of (63) are ultimately quite similar to previous studies, merely in a different setting. When the authors dug deeper into this system in (83), they found something that adds more significantly to the entire story. In Figure 6 we see the same two dimensional porous medium as above along with the trajectory of a single advective particle superimposed. Below are the time series along that trajectory for the particle's velocity and acceleration.

Looking carefully at these series, the Lagrangian acceleration displays

an intermittent behavior as it switches between periods of low variability to periods with strong fluctuations in magnitude. The low variability regime corresponds to when a particle is in low velocity regions; here Lagrangian longitudinal velocities and accelerations are small and strongly correlated. The large fluctuation regime occurs when the particle is in regions of high velocity such as flow channels where accelerations are large and erratic.

Intermittency is a phenomenon that is observed in many physical settings (e.g. 84), but some key and unique aspects exist in the context of porous media. Some insight can be gained by considering the correlation function of the Lagrangian acceleration as well as that of its absolute value, respectively given by

$$\chi_a(\tau) = \frac{\langle [a(t+\tau) - \langle a \rangle][a(t+\tau) - \langle a \rangle]}{\sigma_a^2} \quad \chi_{|a|}(\tau) = \frac{\langle [|a(t+\tau)| - \langle |a| \rangle][|a(t+\tau)| - \langle |a| \rangle]}{\sigma_{|a|}^2}, \tag{16}$$

where a denotes acceleration. A related and useful measure that is often studied in intermittent systems is the Lagrangian velocity increment associated with some time lag τ, given by

$$\Delta_\tau v = v(t+\tau) - v(t) \tag{17}$$

or better said the distribution of these accelerations normalized by its standard deviation $P(\Delta_\tau v / \sigma_{\Delta v}(\tau))$.

Both of these metrics are displayed for the considered system in Figure 7. For the case of acceleration, the correlation decreases rapidly in time, briefly becoming anti-correlated, due to the rapid fluctuations in acceleration in high velocity channels noted above in Figure 6. On the other hand the correlation

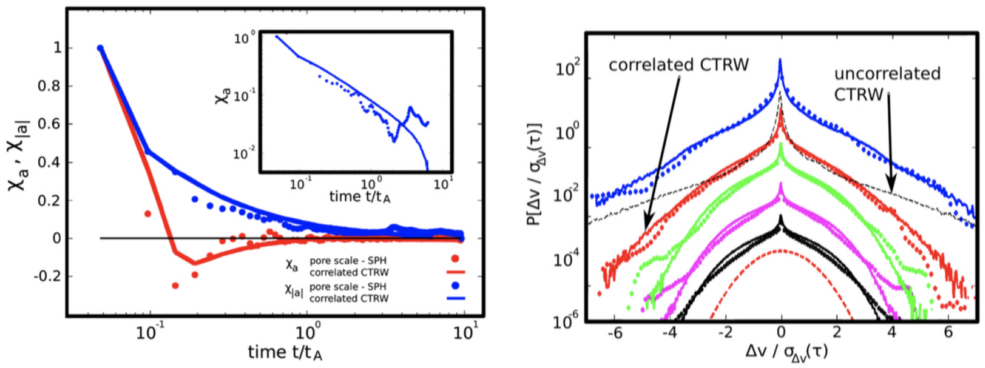

Figure 7: (Left) de Anna *et al.* (83) compared the correlation in acceleration and absolute acceleration for pore scale simulations and a correlated CTRW. The correlation of absolute acceleration is shown in the inset. (Right) The distributions of Lagrangian longitudinal velocity increments at different time lags. As the time lag increases, the distribution approaches Gaussian (dashed line). Adapted with permission from (83).

for absolute value of acceleration decays more slowly showing something more like a power law decay over the observed timescales. In other systems, such as turbulent flows, intermittency is associated with an exponential decay in correlation of $|a|$, which in turn leads to a rapid convergence to Gaussian like behavior. As such, this persistence is a unique and important aspect of intermittency in porous media. Its persistence highlights why it is important to consider, as anomalous effects may play a role for longer times than assumed in conventional models. The distribution of Lagrangian velocity increments at fixed time lags has a sharp peak around 0 with symmetric exponential tails, whose slope increases as the lag increases. The sharp peak in the center is associated with low velocity regions that correspond to small accelerations as seen in Figure 6. Such a peak is typically not seen in other intermittent systems such as turbulent flows, where the time varying nature of the flow allows particles to sample velocities more quickly. Also shown in the figure is the Gaussian distribution which would arise at asymptotic times, but that is never obtained here, once again highlighting the persistence of intermittency and anomalous behavior. The observations from this study suggest that any upscaled model for transport should ideally capture these behaviors in accelerations in order to be able to replicate intermittent behavior with these specific characteristics. De Anna *et al.* (83) proposed that the SMM is such a model.

A clear definition of acceleration for comparison with these observation is not obvious in the context of the SMM and so (83) suggested the following. The acceleration during step n, considering spatial increment λ and time increment τ, can be seen as

$$\lambda = v_{n-1}\tau_n + \int_{t_n}^{t_n+\tau_n} \int_{t_n}^{t'} a_n dt'' dt'. \tag{18}$$

Assuming a constant acceleration over each step and continuity of velocity at turning points

$$a_n = \frac{2\lambda}{\tau_n^2} - \frac{2v_{n-1}}{\tau_n} \qquad v_n = v_{n-1} + a_n\tau_n. \tag{19}$$

With this they were able to compare to observations from the full pore scale simulations. The SMM is able to accurately represent both the correlation of the acceleration and absolute value of acceleration, including anticorrelation and long range effects, as shown in Figure 7. Likewise the distribution of velocity increments for different time lags are in excellent agreement for all considered time lags with peaks and tails well represented. For comparison, a single example for an uncorrelated model is also included. Such a model leads to an overestimate of probabilities of large increments over small lag times, allowing particles to switch velocities too quickly relative to what happens in the real incompressible flow.

The setting considered by (63) and (83) is a highly idealized porous medium relative to what a real geologic medium might look like. To explore whether their findings extended to more realistic systems, the model has been applied to predict solute transport (61) in an image-based reconstruction of a real rock system. Their flow field is shown in Figure 8 along with velocity and acceleration time series in both longitudinal and transverse directions. These time series display the same intermittent behavior as reported in (83). They found that transport is highly anomalous, observing superdiffusive spreading in the longitudinal direction and subdiffusive spread-

ing in the transverse one, again reflecting a balance that likely arises due to the incompressible nature of the flow. In this system they also show that an SMM can faithfully reproduce the behavior measured from their DNS both in terms of temporal scaling of spatial moments and instantaneous distributions of particle locations at various times.

It is important to note that the intermittency discussed in this section applies to time series such as those shown in Figures 6 and 8. However, if one looks at spatial series, that is velocities of particles over fixed spatial increments, a pretty regular spatial signal emerges, where the velocity appears to remain roughly constant/correlated for over an (almost) constant distance; see (85) Figure 2 for a clear example. Such observations again justify the choice of a spatial over temporal Markov model, validating Le Borgne *et al.*'s (20; 48) original observations and suggestions.

3.4. Transport in periodic domains

Many of the classical upscaling theories that are commonly applied in the context of porous media typically rely on the assumption of some representative elementary volume that is assumed periodic in order to close the resulting mathematical system (e.g. 9; 10). While the SMM does not appear to explicitly require such an assumption, a reasonable question is whether it can perform well in such a context also. In particular, many of these classical theories are only valid at asymptotic times and it is often desirable to make predictions at pre-asymptotic times. While these theories can be generalized to pre-asymptotic times, the resulting set of differential equations can be highly nonlocal in space and time and almost as difficult to solve as the full microscale problem as noted by (86; 87). Note that a recent paper (88)

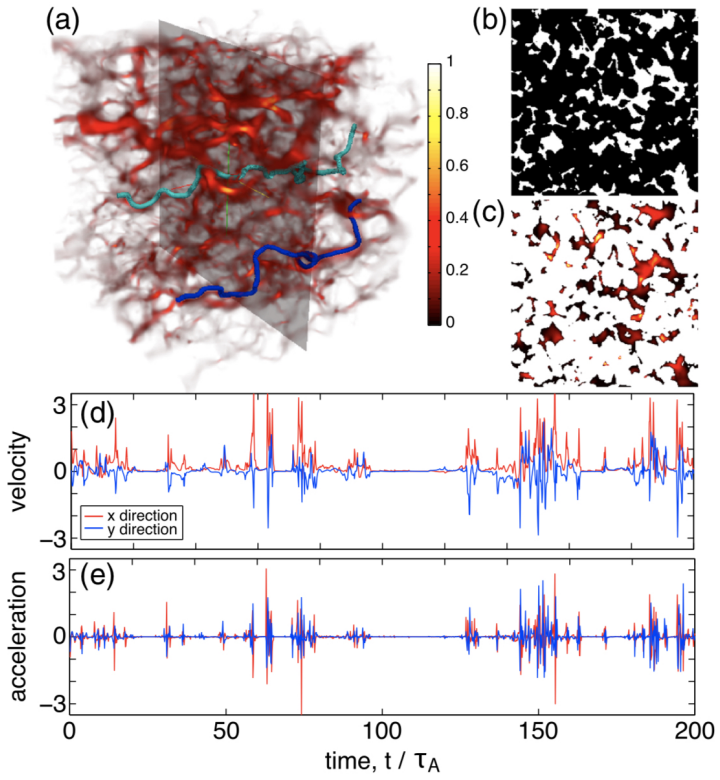

Figure 8: The normalized Eulerian velocity magnitude field through a Berea sandstone sample, with particle trajectories colored blue and cyan (a). (b) and (c) cross sections of the sandstone's pore space (white) and velocity field, respectively. Average porosity is 18.5%. (d) and (e) show the time series of velocity and acceleration for the blue particle trajectory in (a). Adapted with permission from (61).

does demonstrate the existence of an REV as a necessary condition for any CTRW. However, this REV is not defined in the traditional sense in terms of medium properties but rather in terms of the representativeness of the Eulerian flow properties.

Recognizing that a periodic domain has a natural length scale, that is the length of the actual cell, (63) proposed that this should be the fixed spatial jump in the SMM equations in (1). In order to test this, they considered a simple benchmark problem that has often been considered as a useful idealization of a porous medium - flow through a periodic channel with a sinusoidal boundary as depicted in 9 (89; 90). One of the reasons that this flow is considered interesting is that it has a fast preferential flow down the center line and depending on the aspect ratio of the pore, as well as the considered Reynolds number, the emergence of recirculation zones, which act as traps causing particles to potentially be retained for long times relative to the main flow. Two simulated trajectories in such a setting are shown in Figure 9, reflecting both a very fast as well as a very slow trajectory. In particular, note that the slow one is repeatedly trapped, while the fast one persists at being fast, suggesting a correlated process similar to the ones we have discussed in the settings above.

In (63) Stokes flow is considered and the system behaves in a very similar manner to the more realistic porous medium discussed above and shown in Figure 5. Later, Bolster *et al.* (72) considered a diverse range of Reynolds numbers to explore the impact of flow inertia on transport in the same periodic geometry. In both studies the authors simulated transport across two periodic elements recording the amount of time it took each particle to tra-

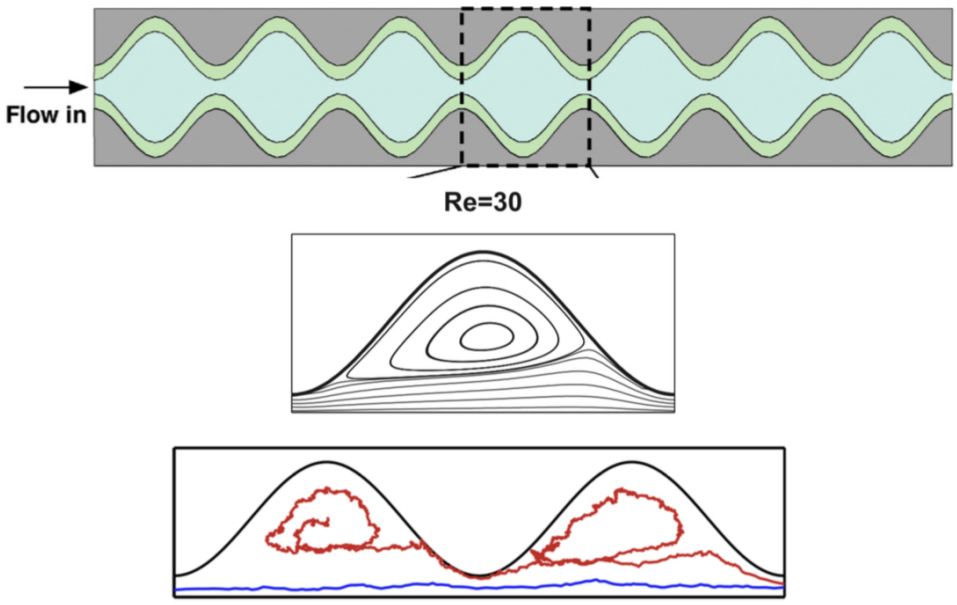

Figure 9: The top figure shows a periodic pore domain, where the dashed line is one representative cell. The middle figure shows the streamlines in the periodic pore for a Reynolds number of $Re = 30$. The bottom figure displays two sample particle trajectories, for a $Pe = 1000, Re = 30$. Particles initialized at the pore throat tend to persist in the main channel, while particles that start in the trapping zone are more likely to enter the trapping zone in the next cell. Adapted with permission from (63).

verse the first and then the second periodic element. From this they measured the transition matrix of the system. In particular, unlike previous studies which predominantly focused on purely advective transport, or only considered one particular Péclet number, these studies explored behavior over a range of Péclet numbers from diffusion to advection dominated. Here the Péclet number is defined as

$$Pe = \frac{2Uh}{D} \tag{20}$$

where U is the mean velocity, h the characteristic half-width of the channel and D the diffusion coefficient. A typical transition matrix for $Pe = 100$ and $Pe = 1000$ is shown in Figure 10. The $Pe = 1000$ case shows the characteristic behavior that we have described in several settings so far - that fast particles are most likely to persist at being fast and that slow particles are most likely to persist at being slow, reflected by the strong diagonal band. Predominance of diagonal terms is much less evident in the $Pe = 100$ case, suggesting that correlation effects here are much less important than for the larger Pe case. Using this result, the authors compared breakthrough curve and moment evolution measured from DNS to predictions using both correlated and uncorrelated CTRW models, where the uncorrelated model draws transition times from the distribution obtained for transition times across a single periodic cell. They found that for all cases of $Pe \leq 100$ that the uncorrelated and correlated models performed equally well, while for $Pe \geq O(100)$ the model that did not include correlation effects failed to reproduce observations, in particular missing early arrivals and late time tails. Samples highlighting this can be seen in the breakthrough curves in Figure 10. This

threshold has been confirmed by other studies also, suggesting that correlation effects should be accounted for any time a system with $Pe > O(100)$ is considered.

An additional question that was addressed by (63) relates to the discrete nature of the transition matrix: how many bins should the transition matrix be discretized into to effectively capture large scale behavior. Via an error analysis, they found that as long as more than ten bins were used, that SMM predictions converged to the reference solution. While this is an entirely empirical observation for an isolated case, it has been found to hold in other settings also (e.g. 91; 92).

As in previous implementations of the SMM for the first set of periodic systems considered (63; 72), parameterization of the model was conducted by simulating particle transport across two periodic elements in order to measure both the transition time as well as the transition matrix. For most other upscaling approaches only one element is typically considered and so some have criticized the SMM as gaining an unfair advantage over other models in this regard. Sund *et al.* (93) realized that in a periodic setting this parameterization could actually be done by simulating transport over only one single periodic element.

The key to their approach was recognizing that a particle's travel time across a single element is dictated by the location where it enters that element. Given its starting point, a particle has a finite range of travel times and exit locations. The exit location can then be used as the inlet location for the next element. This is depicted pictorially in Figure 11, where trajectories are shown for three different start locations across one periodic element

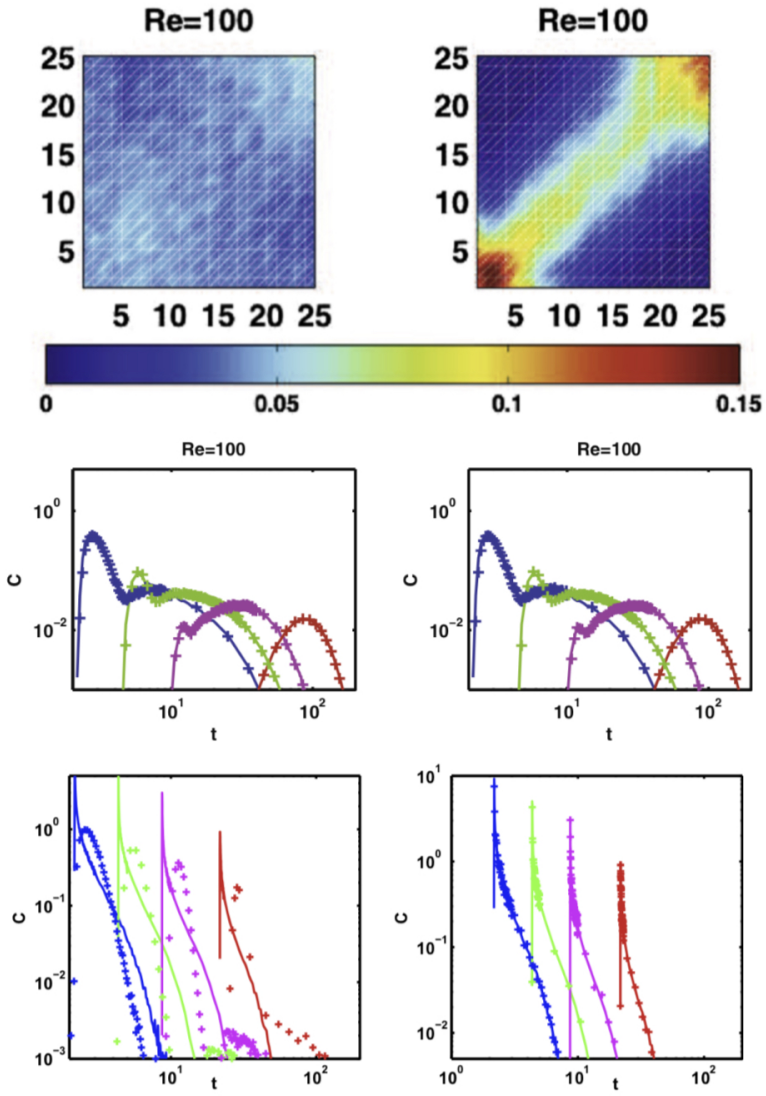

Figure 10: (Top row) Transition matrices for a periodic pore domain for $Pe = 100$ (left) and $Pe = 1000$ (right) for a flow with Re=100. Correlation strength increases with increasing Pe. (Middle row) shows uncorrelated CTRW (left) and SMM (right) predictions vs DNS (solid lines) of the periodic pore domain at $Pe = 100$. The bottom row shows uncorrelated CTRW (left) and SMM (right) predictions vs DNS (solid lines) at $Pe = 1000$. Adapted with permission from (72).

for two different Péclet numbers ($Pe = 100$ and 1000). For the lower value of Pe there are a broad range of possible outlet locations with significant overlap between the three distinct starting points. On the other hand, for the higher Pe the range of possible outlet locations is much tighter, inducing the correlation. An effective transition matrix is also shown for the two cases highlighting probability inlet versus outlet location, with very similar structural features to that which relates travel times in Figure 10. Note that this transition matrix is for illustration purposes only as it is never explicitly used.

The parameterization for this novel approach is developed by simulating trajectories for N_{PS} particles distributed across all possible inlet locations. With this, one can define a set of $\mathcal{S} = \{s_1, \ldots, s_{N_{PS}}\}$ of trajectories s_i, each of which travels from an inlet to an outlet location. Each trajectory s_i has an associated inlet location $y_{in}(s_i)$, an outlet location $y_{out}(s_i)$ and a travel time $\tau(s_i)$. A specific order of the trajectories s_i is assumed by setting $y_{in}(s_1) < y_{in}(s_2) < \ldots < y_{in}(s_{N_{PS}})$. For computational reasons, the trajectories are subdivided into a number of N_{bin} subsets (similar to the discretization of the transition matrix),

$$\mathcal{S}(j_{bin}) = \{s_i \in \mathcal{S} : y_{in}\left(s_{jb-}\right) \leq y_{in}\left(s_i\right) \leq y_{in}\left(s_{jb+}\right)\}, \tag{21}$$

where

$$j_{b-} = \left(\frac{j_{bin} - 1}{N_{bin}}\right) N_{PS} + 1; \quad j_{b+} = \frac{j_{bin}}{N_{bin}} N_{PS}; \quad j_{bin} = 1, \ldots, N_{bin}. \tag{22}$$

This sets a mapping between a location y_{in} at the inlet section and a bin number j_{bin}, which establishes a direct link between the location of the

particle at the inlet section and the travel time through the trajectory s_i. As noted, the outlet position associated with trajectory s_i serves as the inlet position for the next transition (or better said, sets the bin from which the next trajectory is sampled). Sund *et al.* (93) chose to study the same geometry as shown in Figure 9. By doing this the authors were able to run a fully parameterized SMM that performed as well as previous versions, but with only half the simulation required for parameterization. Additionally, the actual implementation of the model is more efficient resulting in an even faster model (since as noted above, no transition matrix step is ever explicitly needed). Finally, as further discussed later in section 5.1, this version of the SMM includes the ability to recover particle spatial distributions within each periodic cell. This trajectory-based framework can be indeed seen as a Lagrangian numerical closure for a model, that can be used to approximate solute mixing and particle positions below the cell resolution, thus retaining close analogy with closure variable invoked in classical Eulerian upscaling approaches.

3.5. Applications to real systems

A criticism of the SMM is that proper parameterization requires extensive data that cannot readily be obtained in field and laboratory settings. In all cases discussed so far this comes from high resolution simulations, which directly measure particle travel times and correlations. Most commonly, particle trajectories are measured over two characteristic lengths in high resolution direct numerical simulations that fully resolve flow and transport across the domain of interest. This then provides sufficient data to quantify velocity transition probabilities. Due to this, most SMM applications have

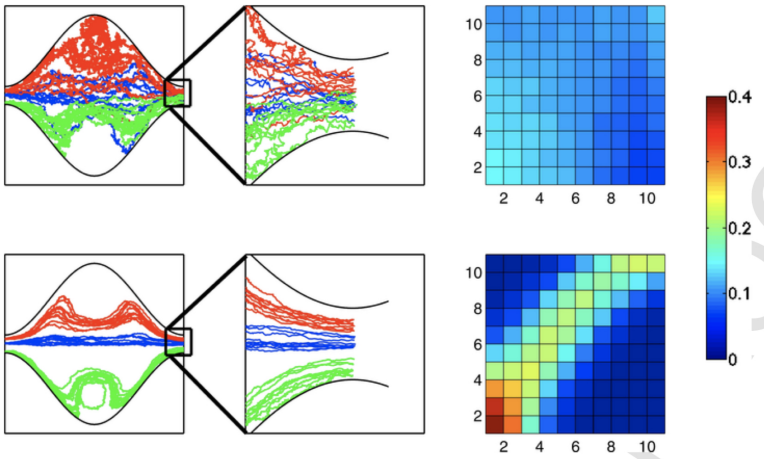

Figure 11: Sample trajectories and the respective transition matrices for particle transport through the periodic pore domain with $Pe = 100$ (top) and $Pe = 1000$ (bottom). Trajectories are initialized in the fast region (blue), intermediate (red), and slow (green) regions of the pore throat. Adapted with permission from (93).

been primarily limited to synthetic numerical systems. Two approaches have emerged recently aiming to overcome these challenges and enable application of the SMM in field-scale and laboratory settings. In the first, Kang *et al.* (74), assume an idealized simplified diagonal transition matrix structure with a single correlation parameter, which can be found by fitting tracer experiments. In the second method, Sherman *et al.* (94) introduce an inverse modeling approach, which infers the transition matrix from two successively measured breakthrough curves. This method was applied using column experimental data to predict transport at the laboratory scale (95). Both of these methods have their associated strengths and weaknesses which are discussed below.

3.5.1. Fractured Media

Kang *et al.* (74) is to our knowledge the first and only study where the SMM is applied to non-synthetic data at the field-scale. The setting that they worked on was experimental data collected from a fractured granite at the Ploemeur field site in France (Figure 12). The matrix permeability within the granite at this site is very low and so groundwater flows primarily through the fracture network, where four major conductive fracture intersections have been identified. Two boreholes, 83m and 100m deep, are spaced apart by a distance $r_c = 6m$, enabling easy injection and extraction of tracer into the network. Kang *et al.* conducted two types of experiments to quantify transport behavior: convergent and push-pull tracer tests. In the convergent tests, a known mass of nonreactive tracer (flourescein) is injected at borehole 1 and tracer concentration is measured at borehole 2. A pump at borehole 2 creates a stationary pressure field driving flow from borehole 1 to 2. In the push-pull tests, a known mass of tracer is again injected into borehole 1 followed by a continuous injection of water for a set amount of time (push). Then a pump at borehole 1 is used to reverse the direction of flow (pull) and the tracer is measured at the point of injection.

In fractured media, the four mechanisms that influence transport are heterogenous advection, matrix diffusion, hydrodynamic dispersion, and adsorption, with heterogenous advection being partially time reversible, while the others are not. For this reason, solute spreading due to heterogenous advection is partially reversed in the push-pull experiments. Therefore, the advective spreading in the push-pull experiments is minimized and the observed breakthrough curves display a narrower distribution than the conver-

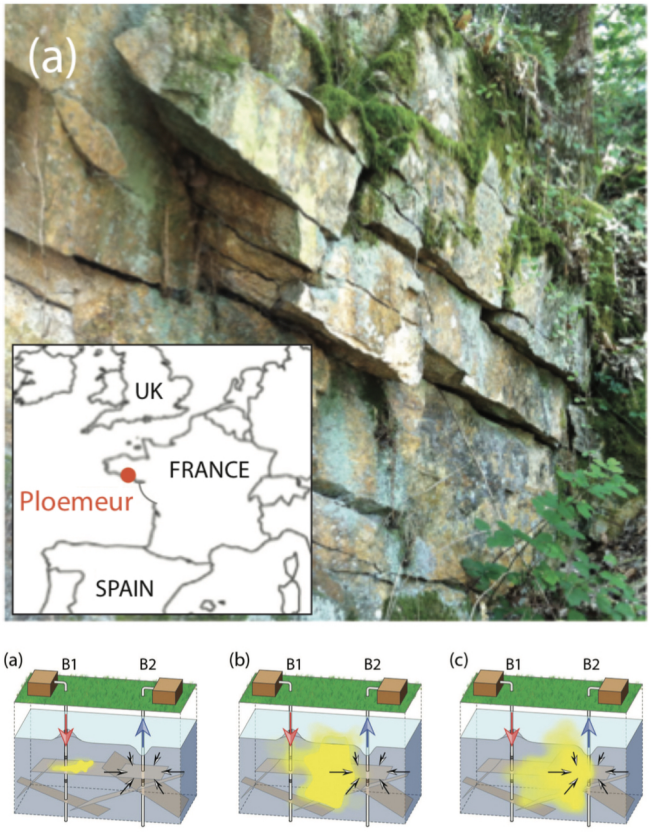

Figure 12: An outcrop of the granite fracture network at the Ploemeur field studied by Kang *et al.* (74). A schematic of the associated convergent test, where a pump drives flow towards borehole 2, tracer is injected at borehole 1 and then measured at borehole 2. Adapted with permission from (74)

gent breakthrough curves, thereby indicating velocity correlation is important in this system. Additionally, the observed breakthrough curves displayed different power-law tailing exponents depending on the fracture upon which tracer was injected, indicative of the varying levels of heterogeneity for each fracture. These heterogeneities, as well as heterogenous advection, must be effectively represented in the SMM for accurate modeling of solute transport through this fractured media.

Kang *et al.* (74) proposed a simplified SMM framework to model the observed transport behavior. To do so, they assume an idealized diagonal transition matrix structure, determined by a single constant parameter a. The idealized transition matrix has diagonal elements with a value a and the remaining elements have equal probability $(1-a)/(N-1)$, where N is the number of matrix columns:

$$T_{ij} = \begin{cases} a & i = j \\ \frac{1-a}{N-1} & i \neq j \end{cases} \qquad i, j = 1..N. \tag{23}$$

a quantifies the probability of persisting in the same velocity class over successive model steps. Note that, as with many empirically measured transition matrices, the fully parameterized transition matrix $\mathbf{T}$ converges to a uniform matrix after many model steps, $[\lim_{n\to\infty} \mathbf{T}^{\,n}]_{i,j} = 1/N$, and thus correlation decays exponentially, specifically correlation at the n^{th} model step is related to the second eigenvalue of $\mathbf{T}$, $C(n) = \chi_2^n = \exp(n \ln(|\chi_2|))$. The second eigenvalue of the diagonalized transition matrix in eq. (23) is $\chi_2 = (Na-1)/(N-1)$. It follows naturally that a dimensionless correlation λ length can be expressed as

$$\lambda = \frac{l}{r_c} \frac{1}{\ln \frac{N-1}{Na-1}} \approx^{N>>1} \frac{l}{r_c} \frac{1}{\ln a^{-1}}. \tag{24}$$

Here l is the streamwise jump distance of the SMM and r_c is a characteristic length between the tracer injection and withdrawal points. This simplified transition matrix of Kang *et al.* (74) allows velocity correlation to be described with a single parameter a, which is related to the correlation length and allows easier parameterization of SMM. Particle motion in the SMM as applied in (74) follows

$$\begin{aligned} r_{n+1} &= r_n + l + \sqrt{2\alpha l}\xi_n \\ t_{n+1} &= t_n + \frac{l r_n}{k_v}\eta_n, \end{aligned} \tag{25}$$

where α is dispersivity, ξ is a identical independently distributed Gaussian random variable, η is a dimensionless time, and k_v is proportional to discharge divided by the fracture aperture. Hence, in addition to λ, the velocity distribution and dispersivity input parameters are required to run the SMM. In this study, the velocity distribution assumed the form of a truncated Pareto distribution with power law slope $1 + \beta$, meaning λ, β and α are the only three parameters that need to be estimated for SMM application.

To this end, random walk equation parameters α (dispersivity), β (velocity distribution), and λ (velocity correlation) were fitted to measured breakthrough curve data. The velocity and dispersivity parameters β, α showed best fit values of $0.75, 0.03$ and $0.85, 0.02$, for two different fractures, respectively. The velocity correlation length was determined to be the same order of magnitude as the mean distance between fracture connections, suggesting that velocities are strongly correlated through a single fracture and decorre-

late at intersections. CTRW model predictions show significant improvement when accounting for velocity correlation, even with this simple idealized correlation structure. Note that the same authors later applied this idealized matrix structure to predict transport observed in numerical simulations of a stressed fracture system with heterogeneous aperture and flow fields (96). The success of the idealized transition matrix structure in both of these systems is exciting for future field SMM applications because it suggests that only certain correlation properties need to be included to faithfully predict transport in certain subsurface media. Furthermore, this simplified structure closely resembles a Bernoulli CTRW, an emerging subclass of SMM models that is discussed further down in section 4.2. We must note that the assumed correlation structure may not reflect universal behavior and therefore it remains an open challenge to fully parameterize the velocity correlation in non-synthetic field scale systems.

3.5.2. Laboratory experiments

One of the challenges with real experimental settings is that detailed information on individual Lagrangian trajectories is not typically available, nor realistically obtainable. Thus directly measuring the transition matrix is next to impossible. In most settings, the best one can hope for is breakthrough curve measurements at multiple downstream locations.

To this end, Sherman *et al.* (94) introduced an inverse modeling approach to estimate the transition matrix from two successive breakthrough curves, specifically breakthrough curves positioned at distances L_c and $2L_c$ from the inlet where a pulse injection is introduced. The inverse modeling procedure solves the discretized form of the governing SMM equation, which requires

that particle travel times sample from a discrete probability distribution. The inverse model, like the forward SMM, assumes that travel time distributions between successive spatial increments L_c are stationary. Therefore, the porous medium is conceptualized as a column of identical cells, analogous to the periodic pore domains presented previously. The travel time distribution for each cell is equivalent to the normalized breakthrough curve at the first cell's outlet. A particle's arrival time at the second cell then must be a combination of two times sampled from this travel time distribution. The inverse model leverages the stationary assumption to find combinations of times sampled from breakthrough curve 1 that equal times measured in breakthrough curve 2. Discretizing breakthrough curves 1 and 2 enables all variables in the discretized SMM equation to be known, except the transition matrix, meaning the transition matrix can be estimated by solving a system of equations.

The governing discretized SMM equation can be expressed as:

$$P(\tilde{\tau_2}) = \Sigma_i \Sigma_{j_{\tilde{\tau_1^a}+\tilde{\tau_1^b}=\tilde{\tau_2}}} P(cell\ 1 \in \tilde{\tau_1^a},\ bin\ i) T_{i,j} P(cell\ 2 \in \tilde{\tau_1^b} | binj) \qquad (26)$$

Here $P(\tilde{\tau_2})$ is the probability associated with arrival times at $x = 2L_c$ within a discrete interval $(\tilde{\tau_2})$, $T_{i,j}$ is an element in the transition matrix, and $\tilde{\tau_1^a}, \tilde{\tau_1^b}$ are discrete time intervals to travel across 1 increment L_c, i.e. within $x = [0, L_c]$ and $x = [L_c, 2L_c]$, respectively.

More simply, this equation states that the probability of a particle arriving at $x = 2L_c$ within the interval $(\tilde{\tau_2})$ is all combinations where the time to traverse $[0, L_c]$ plus the time to traverse $[L_c, 2L_c]$ lies in $(\tilde{\tau_2})$. Converting breakthrough curves into discrete distributions means that each discrete arrival time interval has an associated empirical probability and can

be sorted by velocity class, i.e. $P(cell\ 1 = \tilde{\tau_1^a},\ bin\ i)$ is known. Assuming spatial stationarity of travel time distributions throughout the domain allows $P(cell\ 2 = \tilde{\tau_1^b}|binj)$ to be calculated from the discretized breakthrough curve at L_c, leaving $T_{i,j}$ as the only unknown in equation 26. Every discrete time from breakthrough curve $2L_c$ has a corresponding equation, which form a system of equations that estimates the transition matrix when solved. Note that when the number of discretized times from breakthrough curve $2L_c$ exceed the number of elements in the transition matrix, the system of equations is overconstrained, as is the case in (95). The overconstrained system is solved with a least squares method and then transition matrix rows are normalized so that their sum is unity.

To date application of this inverse model has been both on synthetic (94) as well as, more excitingly, a non-synthetic experimental system (95). In (95) transport of a conservative solute through a 1.2 m long column packed with zeolite clinoptilolite, a material with multiscale porosity known to yield anomalous transport, is measured. A pulse of NaCl tracer was injected at the column inlet and breakthrough curve data was obtained at $\frac{1}{6}$, $\frac{2}{6}$ and $\frac{5}{6}$ the column's length. Experiments were run at $Pe \sim O(100), O(1000)$ in triplicate. A schematic of the experimental setup is shown in Figure 13. Breakthrough curves sampled at the first two ports were discretized, then fed into the inverse algorithm, and the transition matrix was estimated. The transition matrix and measured breakthrough curves parameterize the forward SMM, enabling breakthrough curve predictions at port 3 to be compared with experimental data.

Correlation was determined important for both Pe numbers as the esti-

mated transition matrices displayed a diagonalized structure, indicating fast velocities preferentially remain fast and slow velocity preferentially remain slow. As expected, correlation increased with increasing Pe. Estimated breakthrough curves using the inferred transition matrix significantly improved upon predictions using an uncorrelated CTRW model as shown in Figure 13. Specifically, both breakthrough curve peak and tailing behavior was better captured when correlation was included for both Pe experiments. As expected in any inverse modeling process, discretization and measurement error in the data induce uncertanties in parameters' estimates (i.e., transition matrix entries) and the inverse method requires further iteration and optimization. (95) did so in a very simple manual manner, obtaining excellent agreement with experimental measurements. Fully automating this secondary optimatization still remains to be done. However, to date and to our knowledge, this remains the only study where a fully parameterized SMM, i.e. where the entire matrix correlation structure is faithfully represented, is applied in a non-synthetic setting.

3.6. Higher Dimension Processes: Training Trajectories in 3-d domains

While a great deal can be learned by studying the idealized periodic pore systems that we have mentioned, it is also important to recognize the limitations. The fact that the system is so simple means that while it may display some of the interesting features of a real porous medium, such as preferential flow channels and trapping regions, these features are of one size unlike a real geologic medium where a broad distribution of channel sizes and trapping regions can exist. Additionally the completely periodic nature of the system is not reflective of subsurface porous media.

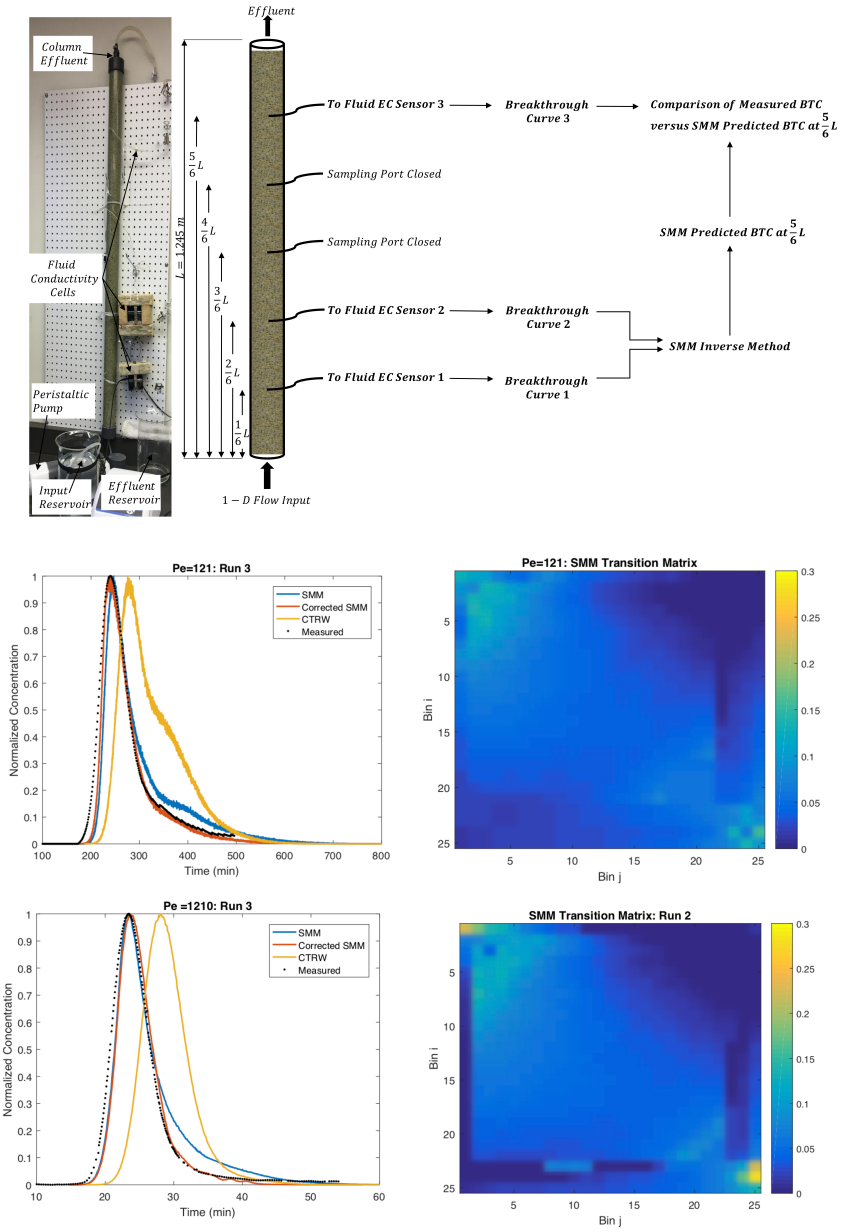

Figure 13: A schematic of the column experiments of Sherman *et al.* (95), where sampling ports 1 and 2 are used to measure breakthrough curves for inverse SMM parameterization and sampling port 5 validates predictions. The model predictions, experimental measurements and transition matrices are shown for $Pe = 120, 1200$. Adapted with permission from (95).

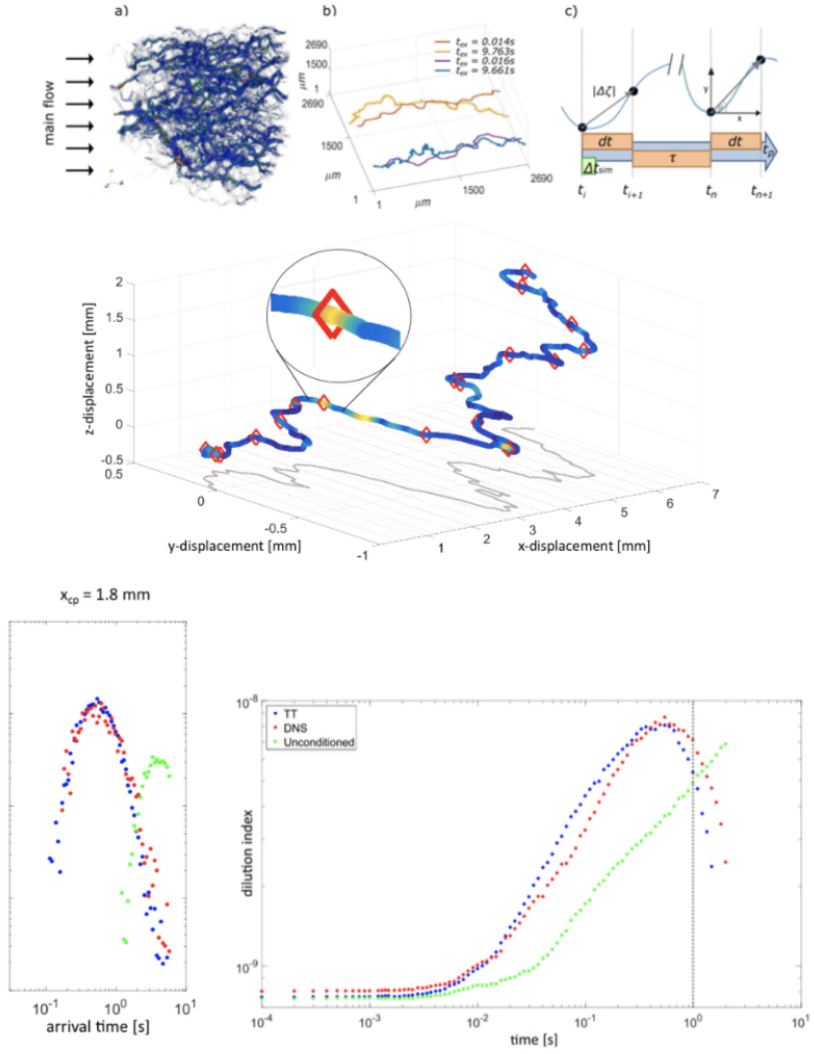

Figure 14: The top figure shows the flow field of the sandstone studied by (122). Sub figure b shows two particle trajectories for $Pe = 10$ (yellow and blue) and $Pe = 100$ (orange and purple). Sub figure c gives a schematic of the Most *et al.* preprocessing procedure. The middle figure displays how a particle trajectory is subdivided by (62), where red diamonds show where the trajectory is divided; the bottom figures are predicted arrival time distributions and dilution index using the training trajectory approach. Adapted with permission from (62)

To overcome some of these limitations and focus on a more realistic system (122) simulated high resolution trajectories through a series of real geologic media (a Doddington Sandstone), whose structure was digitally mapped using high CT scanning. The velocity field and representative trajectories are shown in Figure 14 (top). Unlike many previous studies they focused not just on the correlations between successive longitudinal jumps, but looked at the full correlation of velocities in all three dimensions of the system, finding that there is a strong cross dependence between longitudinal and transverse increments. Based on an extensive empirical analysis of the 3-d trajectories, they concluded that i) memory and cross dependence are persistent in and among all directions, ii) that the dependence is highly-nonlinear, iii) that this co-dependency occurs at different temporal scales, and iv) that it is dependent on the Péclet number. Their work suggests that should one want to extend the SMM to predict realistic concentration fields in three-dimensions that one would need to thoroughly describe the governing statistics of a three-dimensional transport problem, which would require parameterization of a nine-dimensional transition matrix. While possible, it requires immense effort and computational power.

Recognizing the practical limitations of a 9-d transition matrix, (62) proposed a novel solution called the training trajectory approach (TTA). In it, the authors take the full length trajectories that are simulated from the DNS (Figure 14) and use these as a library of plausible paths. Each trajectory is divided into equidistant segments of length as depicted in the middle row of Figure 14. The segments are stored in a database, from which the increments for the SMM model are sampled, giving a transition time and displacement

direction. The key difference is that this decomposes the 3-d transport into a series of steps that are also 3-d, but the steps in the Cartesian directions are not simulated independently, so the 9-d transition matrices are avoided entirely. The necessary assumption is that this archive of training trajectories inherently captures all the processes and correlations required to represent larger scale transport. (62) provide extensive criteria required to ensure this and for a comprehensive discussion we direct the interested reader there.

4. Velocity Transition Models

The previous section highlighted empirical approaches to modeling the transition matrix, reflecting much of the early work in the field. More recently, theoretical frameworks based on analytical velocity transition models have emerged. These are the focus of this section. In general, the velocity field in steady, divergence-free flows often satisfies the stationary assumption. However, particle transport through both fractured and porous media has been found to be quite sensitive to the initial Lagrangian velocity distribution (97; 98). Therefore, a CTRW framework must properly account for the spatial evolution of the initial Lagrangian velocity. To this end, random walks through velocity space have emerged to characterize the Lagrangian velocity evolution through disordered media, while still invoking a spatial Markov process.

Dentz *et al.* (99) studied the evolution of Lagrangian velocity statistics and developed a Markov chain CTRW that accounts for such evolution with a stochastic relaxation process. To do so, the authors established a relationship between the Lagrangian and Eulerian velocity fields, showing that any

Lagrangian velocity distribution evolves to the flux-weighted Eulerian distribution for ergodic systems. Here, we highlight some key arguments of Dentz *et al.* that lay the framework for velocity space random walks.

In the absence of diffusion, particle trajectories through a heterogeneous steady velocity field $\mathbf{u}(\mathbf{x})$ is described with the advection-equation:

$$\frac{d\mathbf{x}(t,\mathbf{a})}{dt} = \mathbf{v}(t,\mathbf{a}) \tag{27}$$

Here $\mathbf{v}(t,\mathbf{a})$ is the Lagrangian velocity, and $\mathbf{a} = \mathbf{x}(t=0,\mathbf{a})$ is the particle location at initial time. Similarly, particle motion can be described along particle trajectories s and in time:

$$\frac{ds(t,\mathbf{a})}{dt} = v_t(t,\mathbf{a}) \qquad \frac{dt(s,\mathbf{a})}{ds} = \frac{1}{v_s(s,\mathbf{a})} \tag{28}$$

$v_t(t,\mathbf{a})$ and $v_s(s,\mathbf{a})$ represent t(ime)-Lagrangian and s(pace)-Lagrangian velocity distributions, respectively, which represent velocities obtained by uniform sampling in time or space. As discussed in the previous sections, the SMM framework is based on the approximation of $v_s(s,\mathbf{a})$.

Consider the absolute Eulerian velocities $v_e(\mathbf{x}) = |\mathbf{u}(\mathbf{x})|$ within the domain volume V. Then the Eulerian PDF is defined through spatial sampling as

$$p_e(v) = \lim_{V\to\infty} \frac{1}{V} \int_\Omega d\mathbf{x}\delta[v - v_e(\mathbf{x})] \tag{29}$$

With these definitions and under certain assumptions, it is possible to link the Eulerian and Lagragian velocity field distributions. By assuming ergodicity of both Eulerian and Lagrangian velocities, sampling Lagrangian velocities along one particle trajectory is equivalent to sampling velocities

for many particles. Sampling particle trajectories can be done over fixed temporal or spatial increments to find the t(ime)-Lagrangian and s(pace)-Lagrangian velocity distributions.

$$p_t(v, \boldsymbol{a}) = \lim_{T \to \infty} \frac{1}{T} \int_0^T dt \; \delta[v - v_t(t, \boldsymbol{a})] \tag{30}$$

$$p_s(v, \boldsymbol{a}) = \lim_{L \to \infty} \frac{1}{L} \int_0^L ds \; \delta[v - v_s(s, \boldsymbol{a})] \tag{31}$$

Here T, L are a sampling time and length, respectively. The Lagrangian ergodic assumption requires that the particle t-velocity distribution is spatially independent and equivalent to the ensemble average over all particles. Additionally, the incompressibility of the flow field and volume conservation requires that the t-sampled and Eulerian velocity distributions are equivalent, $p_t(v) \equiv p_e(v)$. Through a variable change of s and t, Dentz *et al.* (99) shows the s-Lagrangian velocity distribution is linked with the t-velocity distribution and thus also the Eulerian velocity distribution by flux-weighting,

$$p_s(v) = \frac{v p_e(v)}{\langle v_e \rangle} \tag{32}$$

Relating the Eulerian and Lagrangian velocity distributions is important as it lays the foundation for random walks through velocity space. Equation (32) indicates that in asymptotic conditions (i.e., distances) the s-Lagrangian velocities converge to flux weighted velocity distributions. It also implies that when the initial Lagrangian velocity distribution does not coincide with the steady state velocity distribution, the Lagrangian velocity distribution evolves along streamlines towards this asymptotic limit, i.e., under ergodic assumptions any Lagrangian velocity distribution evolves to the flux weighted

Eulerian distribution given that sampling temporal/spatial scales can sufficiently represent all fluctuations in the global flow field.

As previously emphasized, flow properties in the subsurface are often strongly correlated in space because of the inherent correlation structure of porous and fractured media. For example (100) quantifies the correlation length of the inverse of v_s, also termed as slowness. These results show that the integral scale of s-Lagrangian velocity can be related to the one of the underlying hydraulic conductivity fields. For velocity distributions resulting from multi-Gaussian conductivity fields, the integral scale of $1/v_s$ decreases with increasing heterogeneity. For $\sigma_Y^2 > 6$ the slowness integral scale converges to 4/3 of the hydraulic conductivity. These results show that it is possible to define an inherent correlation length to model transport velocity through a Markov chain, exploiting the emerging correlation.

In other words, it is reasonable to define a characteristic correlation length scale l_c for which velocities persist. Given l_c, the characteristic time of particle velocity persistence is l_c/v_t. This implies that small velocities will persist for longer times than fast velocities and is consistent with the earlier discussion on intermittent behavior: relatively long temporal durations of slow velocities are mixed with sudden abrupt and short lived high velocities periods. The characteristic length scale l_c naturally informs implementation of random walk models; a correlated random walk model will only be useful when model spatial jump lengths are smaller than l_c, $\Delta s << l_c$. Lag distance Δs needs to be large enough to capture correlation properties, but sufficiently small such that successive models steps remain correlated.

The equations describing particle motion in velocity space are as follows:

$$\begin{aligned} s_{n+1} &= s_n + \Delta s \\ t(s_{n+1}) &= t(s_n) + \frac{\Delta s}{v_s(s_n)} \end{aligned} \tag{33}$$

Here Δs is a spatial increment along a particle pathline. Multiple frameworks have emerged for random walks in velocity space that model the evolution of velocity along a particle trajectory, following the above framework. To this end, two methodologies were extensively applied by Dentz and co-workers and are discussed here, i.e., an Orstein-Uhlenbeck process and a Bernoulli CTRW framework.

4.1. Ornstein-Uhlenbeck Process

The Ornstein-Uhlenbeck framework is a classical formalism to express transport through a Markov process and has been applied throughout the physics literature for about a century (101). The reasons for the success of this approach have been extensively reported in the literature, e.g. (102; 103). In the context of our discussion a relevant feature of the OU framework is that it naturally describes relaxation to an asymptotic state through a Markov chain, and that it incorporates fluctuations around a stable state through linearization. The OU framework therefore provides an ideal candidate to ground the parameterization of the s-Lagrangian velocities through a SMM.

Morales *et al.* (98) experimentally traced flow particles in a transparent three-dimensional porous medium using particle tracking velocimetry (PTV) methods, which allowed them to quantify correlation and velocity evolution. The particle velocity distribution evolved from an initial to steady state distribution, which were accurately approximated with a lognormal distribution.

A benefit of a lognormal distribution is that the log-velocity steady state distribution $w_s(s) = \ln(v_s(s))$ is Gaussian,. The evolution of a particle's log velocity can be then modeled as an Ornstein-Uhlenbeck process such that

$$w_{n+1} = w_n - \frac{\Delta s}{l_c}(w_n - M_s) + \sqrt{\frac{2\Sigma_s^2 \Delta s}{l_c}}\eta_n \qquad (34)$$
$$t_{n+1} = t_n + \Delta s \exp(-w_n)$$

where M and Σ are related to the mean and variance of the velocity distribution and η is a random number drawn from a standard Gaussian. The Gaussian variable simulates subpore scale fluctuations of the velocity magnitude. In the presence of general (i.e., non lognormal and non gaussian) velocity distributions, the scores $w(s)$ can be defined through a transformation

$$w(s) = \Phi^{-1}(P_s[v_s(s)]) \qquad (35)$$

where $\Phi(w)$ and $P_s(v)$ represent unit Gaussian and v_s cumulative distribution functions, respectively. After approximating the OU process through (34) the velocity is obtained as $v_s(s) = P_s^{-1}\{\Phi[w(s)]\}$. The velocity is persistent over Δs, i.e. $w_s(s)$ decays exponentially $\exp(-s/l_c)$ and Δs satisfies the $\Delta s << l_c$ constraint. Note through PTV all model input parameters in (34) can be measured experimentally.

Morales *et al.* (98) demonstrated that this Ornstein-Uhlenbeck spatial Markov framework captured intermittent behavior and the velocity distributions at all time scales, as observed in their laboratory PTV experiments. The OU SMM simulated isochronal particle trajectories faithfully reproduced the magnitude and duration of high velocity events as measured by the PTV t-Lagrangian particles velocities, meaning that the velocity distribution and

intermittent behavior is captured at all time scales.

Puyguiraud *et al.* (85; 104) demonstrated that the Ornstein-Uhlenbeck SMM correctly predicts the evolution of the s-Lagrangian distribution in pore scale numerical simulations of transport through a Berea sandstone sample over a range of time scales. This OU approach enables the evolution of non-stationary velocity statistics and intermittent behavior to be faithfully modeled, which in turn means that pre-asymptotic behavior is well represented. OU SMM approaches therefore have exciting potential applications in many environmental flows, where Lagrangian velocity statistics display intermittent behavior and non-stationarity over a range of scales. A benefit of this framework is that it is parameterized with only the global Lagrangian velocity distribution, which is related to the Eulerian velocity distribution, and a characteristic length scale, which (85) found is the same order of magnitude as the characteristic pore scale. Hence the model does not require extensive Lagrangian data for parameterization, which has been a limitation of most commonly used SMM frameworks.

4.2. Bernoulli CTRW

Assuming that velocity transitions via a Bernoulli process is another method to capture intermittent behavior and model the evolution of velocity statistics along particle streamlines (99; 105; 106; 107; 85; 104). In a Bernoulli framework, particles transition through time and space according to eq. (33). Velocity correlation is captured by assuming velocity follows a Bernoulli process, i.e. particle velocity persists from the last model step with probability P and samples a new velocity otherwise with probability $1 - P$; hence particle trajectories are still conceptualized as a spatial markov

process. Dentz *et al.* (99) first proposed a Bernoulli framework, where the s-Lagrangian velocity series is modeled as:

$$v_s(s + \Delta s) = [1 - \xi(s)]v(s) + \xi(s)\nu(s) \tag{36}$$

where ξ is a Bernoulli variable that returns 1 with P and $\nu(s)$ are identically independently distributed velocities that sample from the steady s-Lagrangian velocity distribution. The value of P can be estimated by assuming that velocity transitions at a constant spatial rate inversely proportional to the correlation length l_c (99; 106; 107) such that $P = \exp(-\Delta s/l_c)$. Note that the Bernoulli CTRW is very similar to the idealized diagonal transition matrix by Kang *et al.* (74; 96), except in their framework sampling from a bin allows particle velocity to fluctuate somewhat even when the Bernoulli variable favors a persistent velocity. The benefit of the Bernoulli CTRW framework is that velocity correlation is parameterized with a correlation velocity scale determined by l_c, and therefore an entire transition matrix is not required. A simple way to estimate l_c is to find the distance where particle velocity anti-correlates as determined by a velocity correlation function.

The Bernoulli CTRW has been successfully applied in both three-dimensional and two-dimensional fracture networks (107; 108). In fracture networks, particle velocity is highly correlated on the fracture scale and then may rapidly transition at a fracture intersection. Hence, the characteristic length scale is on the same order of magnitude as the mean fracture length. Such a Bernoulli CTRW framework has been applied to accurately reproduce breakthrough curves generated from 3D numerical simulations of stochastically generated networks whose fracture radii followed a power law distribution (107) and 2D geologically mapped fracture networks under different stress conditions

(108). In these studies, an additional tortuosity parameter was introduced to account for the fact that the multi-dimensional network structure allows for particle motion in transverse directions and so the advective distance a particle travels is greater than the linear distance in the primary flow direction. This added distance delays downstream solute breakthrough, meaning the travel time between model steps in (33) must be modified via a tortuosity parameter χ_s:

$$\begin{aligned} x_{n+1} &= x_n + \Delta x \\ t(x_{n+1}) &= t(x_n) + \frac{\chi_s \Delta x}{v_s}. \end{aligned} \tag{37}$$

Here, particle velocity transitions along streamlines, but traverses only in x-space, the direction of primary flow, because longitudinal spreading is of primary interest. χ_s is an effective tortuosity parameter that corrects particle travel distances, accounting for transverse excursions, and thereby delays effective transport. In these studies χ_s is calculated as the mean particle pathline distance divided by the total linear distance in the primary flow direction. Note that other definitions of tortuosity, such as the ratio of the mean velocity norm over the mean velocity in the mean flow direction are also commonly used (109; 110) and, for volumes that are large enough, equivalent to this definition. Hyman *et al.* (107) demonstrated the Bernoulli CTRW model accurately captures breakthrough curve tailing behavior for networks whose fracture radii are sampled from power law distributions with varying power law slopes and showed that model accuracy improves when initializing the particle velocities with the inlet velocity distribution. Kang *et al.* uncovered that under specific stress conditions, the correlation length scale is correlated with velocity and proposed a dual correlation length Bernoulli CTRW, i.e.

P is dependent on velocity. The authors applied this dual correlation length Bernoulli to predict breakthrough curves in complex 2D networks. These findings agree with a study by (85), who found that the convergence rate for velocity evolution in numerical simulated Berea sandstone is velocity dependent. Note that in heterogeneous fractured media, a transition matrix may be spatially dependent due to the heterogeneity of the network structure at the scales of interests, meaning using the traditional SMM parameterized from two initial cells may impose false correlation structures on transport behavior. The Bernoulli CTRW framework, simply assumes that velocities transition over a characteristic length related to fracture radii, which relaxes the correlation structure and therefore is more suitable in this context.

Bernoulli CTRWs have also been applied to model transport through porous media (85; 111). Carrel *et al.* (111) applied a Bernoulli CTRW to model transport processes through a porous media with varying degrees of biofilm growth. To do so, Nafion pellets were added to a bacterial inoculum, which were packed in a saturated flow cell to create a porous medium. The medium was saturated with glucose aqueous solution, thereby promoting biofilm growth in the flow cell. Fluoresecent tracer particles were seeded in the flow and tracked through time with particle tracking velocimetry (PTV), enabling t-Lagrangian velocity distributions to be quantified for different periods of biofilm growth. Particle trajectories displayed intermittent behavior, and larger biofilm growth resulted in fewer channels in the flow structure and increased average longitudinal velocity because porosity progressively decreased with increased growth. The Lagrangian trajectories enabled velocity correlations to be quantified, which was shown to increase with in-

creased biofilm growth. Transport through each biofilm snapshot was modeled with a Bernoulli CTRW, where velocities moved along streamlines and $P = \exp(-\Delta s/2\lambda)$, where exponential decorrelation occurs over twice the correlation length and the correlation length is found as the integral of a correlation function. Note that the characteristic length scale is similar to that found in (85), which was 2.5 times the average pore length. Bernoulli CTRW predictions for mean and centered mean squared displacements (MSD) are in good agreements with PTV measurements and the MSD exponent increased with biofilm growth, suggesting increasing biofilm growth causes an increase in anomalous transport, which is consistent with observations in other settings also (e.g. stream beds 4). Again, the study demonstrates the exciting potential of a Bernoulli CTRW framework, as it faithfully captures anomalous transport at the pore scale without requiring as extensive a parameterization process as measurement of a full transition matrix.

5. Mixing and Reactions

The primary goal of most of the cases presented so far has been to describe, or predict, the mean transport behavior as a 1-d, upscaled approximation. The simplification to 1-d is practical in the context of subsurface hydrogeological systems because the inaccessibility of the subsurface introduces significant uncertainty in the 3-d architecture, making precise simulations impossible, but also because observations are not abundant. Consider that the most reliable data about subsurface conditions comes from boreholes, which are vertically averaged samples at fixed points. It is possible to simulate, and verify, an upscaled model at these points but there are many relevant appli-

cations where knowledge of a concentration field, or its variance about the mean, are necessary, instead of time series of concentration at a point. For example, mixing and chemical reactions depend on local concentrations and concentration gradients (e.g. 112; 113), meaning that an average concentration is not sufficient to make an accurate prediction. In order to be useful for such problems, the SMM would need to be able to represent concentration fluctuations in an effective manner. This section describes some recent work, much of it still in early developmental stages, that has begun to explore how to do so efficiently.

5.1. Studies in Periodic Domains

Describing mixing in a Lagrangian sense generally means estimating specific particle positions over time, instead of estimating total travel times. Sund *et al.* (93), who proposed the trajectory based SMM in periodic domains, suggested that one could make an educated guess as to a particle's specific location if some additional information was stored on each trajectory. The goal is to provide a method for downscaling that enables a more complete representation of the spatially variable concentration field and its fluctuations, enabling the calculation of mixing measures.

The approach used by (93) was to store a discrete form of each trajectory s_i. For each trajectory the discretized counterpart can be defined as

$$\mathbf{P}\left(s_i\right) = \begin{bmatrix} \chi_1 & \chi_2 & \cdots & \chi_n \\ \eta_1 & \eta_2 & \cdots & \eta_n \end{bmatrix}, \tag{38}$$

where the pairs $\left(\chi, \eta\right)_\omega$ identify locations along trajectory s_i, at travel time $\frac{\omega}{n}\tau\left(s_i\right)$, with $\omega = 1, \ldots, n$, and n is the number of intervals that build the

trajectory (see Figure 15a where blue dots show the locations χ_i, η_i along a single trajectory). The collection of points that defined each trajectory were then used to downscale the SMM model by linearly interpolating the particle positions between those stored in $\mathbf{P}(s_i)$, providing a spatially explicit description of particle positions at all times.

The model was developed and tested in a simple periodic pore scale setting. The authors compared measurements from direct numerical simulations and their modified SMM to evaluate predictions of two nonlinear global measures of mixing, generally considered to be necessary for the accurate upscaling of mixing-driven chemical reactions. These are the dilution index (or entropy) $E(t)$ and integral of squared concentration $M(t)$, respectively defined as

$$E(t) = \exp\left(-\int_\Omega p(\mathbf{x},t)\log p(\mathbf{x},t)d\Omega \right) \qquad M(t) = \int_\Omega p^2(\mathbf{x},t)d\Omega \tag{39}$$

The DNS results and the modified SMM were compared at two different Péclet numbers ($Pe = 100$ and 1000) using the downscaling procedure exemplified in Figure 15. The agreement between the two was excellent over all times considered, suggesting that this procedure can effectively model mixing and dilution processes, at least in a global sense, thereby providing a significant expansion of the simulation capabilities of the SMM.

The rates of many thermodynamically favorable reactions in porous media are limited by mixing rates in porous media. This implies that one can use simplified reactions to study mixing instead of the complex multi-component geochemical systems in natural systems. One of the most commonly studied, simplified models is the irreversible, bi-molecular, mixing driven reaction

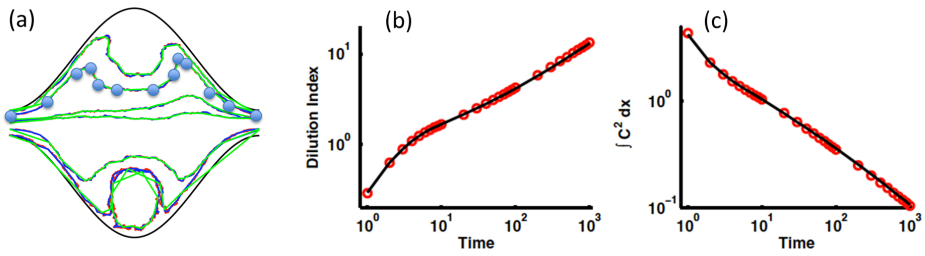

Figure 15: Graphical illustration (a) of the algorithm proposed by Sund *et al.* (93) to downscale particle trajectories and SMM predictions (red) of the dilution index (b) and second concentration moment (c) vs DNS (solid lines) using the proposed downscaling algorithm with $Pe = 1000$; similar agreement is found for $Pe = 100$ (not shown). Adapted with permission from (93).

given by $A + B \rightarrow C$, where the letters denote generic chemical components. (114) adopted this reaction in a periodic domain made up of packed cylinders and proposed a scheme with Lagrangian transport and Eulerian reaction rates stemming from volume averaging. Their proposed model takes advantage of the fact that the SMM can be used to provide accurate predictions of transport, but existing Eulerian approximations can be used for mixing-limited reactions since they do not require the computationally costly calculations of particle-particle interactions (e.g. 115; 116; 117). The approach was shown to be effective for representing subscale fluctuations in concentration fields and, as such, it was also able to accurately predict the amount of product C that is produced. Note that the downscaling approaches in (93) and (114) have some slight differences, but conceptually they are very similar and interested readers are referred to those papers for more details.

Another family of reactions that are very important in the context of

geologic media are surface reactions, which are any reactions that involve mobile phases which directly interact with the liquid-solid surface within a porous medium. Examples include sorption and desorption processes, where a solute can be temporarily (or permanently) trapped relative to the flowing fluid, or biological reactions where bio-organisms living on the surface consume nutrients in the water, removing them permanently from the flow, among many others. Under the assumption of dilute conditions, these reactions can be modeled using linear approximations so they are amenable to the SMM framework without the need for downscaling.

Sund *et al.* (118) considered the same periodic pore system as in Figure 9, but included a hypothetical biofilm layer that particles could diffuse into, where particles were consumed according to a first-order rate law while in the biofilm layer. This study showed that the main effect of biofilm reactions was to truncate the late times in travel time distributions, as these are the ones that spend most time in the biofilm and thus are most likely to react. The travel time distribution for this system was split into two parts - one that accounted for particles that "survive" and another that represented a state of limbo (equivalent to an infinite residence time). The results again showed that accounting for correlations was critical to ensure that fast particles persist at being fast and thus are also more likely to stay alive, while slower particles are more likely to become stuck in limbo. One difference that they found relative to the conservative transport case is that accounting for correlation effects remained somewhat important even at $Pe = 100$, meaning that the sensitivity to correlation effects changes when reactions are involved. Sherman *et al.*(119) came to a similar conclusion when study-

ing sorption-desorption reactions in a similar system. In this case, particles that hit the liquid-solid boundary have a finite probability of being trapped (depending on a first order adsorption rate) and being trapped for a finite amount of time (depending on a desorption rate). Following the trajectory approach developed by (93), the number of times a given trajectory strikes the liquid-solid boundary was added as an additional piece of information in the model and combined with the approach proposed by (120) to link reaction probabilities with sorption rates. Accounting for the number of impacts proved to be sufficient to transform a simulation of conservative transport into one with probabilistic adsorption-desorption. The main difference is that the latter adds delays to the conservative transition times based on the rates of adsorption, desorption and the number of times a trajectory strikes the liquid-solid boundary where the reactive process is taking place. Later (121) applied the model to a more complex non-periodic porous medium.

6. Discussion

So far this paper has reviewed and summarized the Spatial Markov Model over the first decade since its introduction to the porous media community by Le Borgne *et al.* (20). The model aims to represent effective (upscaled) transport in complex porous media from pore- to geologic-scales by building on previous modeling studies that demonstrated the importance of accounting for correlation effects. While the SMM has already shown great promise and evolved immensely in that time, it is still a work in progress and we are excited to see where the next steps will take us. In this final discussion, we highlight some of the primary challenges and limitations of SMMs in their

current forms as well as propose our personal views on pathways forward.

6.1. Challenges and limitations

- Applications to real systems and real data: Two examples were highlighted where the SMM was applied to two sets of real data: a field-based study (74) and a laboratory study (95). The experiments of (95) were in an idealized setting, a 1-d column, but, even in such a controlled environment, additional steps were still needed to optimize the fit of the SMM model to the data. The example of (74) used a site with an uncommon level of characterization developed over years of meticulous data collection, and the transport experiments were designed using this knowledge. While the models could have fit the data well without this characterization, interpretation of the results and success were significantly aided by it. While theoretical studies are advancing fast towards predictive approaches there is still an important gap between the information required to constrain the model parameters and what is typically available in field scale scenarios. Recent efforts based on velocity CTRW (85) require knowledge of the Eulerian velocity pdf of the system to predict transport. This information would rarely be available in a real field setting. The vast majority of SMM applications have relied on high resolution numerical simulations, most of which are a far cry from "typical" field conditions. So, there is a clear need for studies designed around the practical limitations of real systems. This includes testing the SMM in settings with limited characterization, incomplete sampling of tracers, and developing new approaches to parameterization that can provide accurate results without requir-

ing abundant information. These approaches will have to encompass uncertainty quantification and sensitivity analyses to assess the impact of the flow model parameterization on transport dynamics, extending current studies (123).

- Stationarity across scales: A defining feature of the SMM compared to previous, popular models for anomalous transport in porous media is that the SMM relaxes the reliance on independent, identically distributed random variables. The justification for this is that it is necessary in order to capture correlation effects, but all the SMM applications to date have contained an embedded assumption of incremental stationarity for the correlations. This assumes that the same transition matrix is valid along the entire SMM path, but this assumption is not consistent with the complex, hierarchical structure of porous media. However, it may be possible to define transition matrices in a "zonal" fashion in order to capture the changes in correlations along the SMM path. Doing so confidently would likely require abundant characterization, but some geostatistical techniques are able to incorporate conceptual data and incorporating those advances into the SMM could help relax the requirement of strict stationarity.

  A related, subtle point is that many of the numerical studies described herein used multi-Gaussian random fields with fixed length scales for their heterogeneity structures, and the models worked well because the assumption of stationarity was valid. The issue is that the evolving length scales of heterogeneity in natural geologic systems are non-stationary. Studies are needed that use realistic, multi-scale hetero-

geneity fields to investigate when the stationarity assumption is valid, when it breaks down, and how to account for systematic changes as new features in the hierarchy are sampled. A recent example attempting to do this is (124), who use the SMM to study transport in a variably saturated watershed, including overland, vadose zone and saturated flow domains, defining unique transition matrices for different parts of the flow domain. While this preliminary study shows some promise much work is needed here.

- Generalization to nonlinear processes: The SMM is generally designed to represent the mean, effective behavior in the evolution of a concentration field, and its simplest forms assume that transport processes are linear. However, many processes in porous media, particularly chemical reactions which are ubiquitous in geologic systems, are highly nonlinear and so simply predicting mean behavior is not sufficient and some knowledge of fluctuations below the support scale is required. Additionally many forms of calculating reactions require calculation of concentrations in fixed volumes, naturally necessitating an Eulerian interpretation with which the SMM must be compatible. Some efforts have been made along these lines; e.g. the trajectory based methods in periodic domains (93; 114) but generalizing these approaches to more realistic complex settings still remains to be done. The training trajectories approach proposed in (62) shows promise in this regard; however, it has currently only been applied in a relatively simple setting and validated at a scale ($O(mm)$) well below typical scales of interest ($O(m - km)$).

- Enhancing predictive power: Perhaps one of the biggest criticisms of transport models in porous media in general is that in order to parameterize the models one typically has to run a transport experiment at the same scale; that is to predict transport one must first measure it. It would be desirable to establish procedures leading to reliable predictions relying only on prior information available about the geologic system (e.g. distribution of permeabilities in space) or at most about the flow (e.g. approximate velocity distribution in space) and from that information alone, predict transport with reasonable uncertainty. This would truly take anomalous transport models to the next level in terms of actually helping solve practical engineering problems in the subsurface environment, but in order to get there the SMM needs to be studied in more diverse settings and the role of uncertainty and sensitivity on its predictions needs to be considered.

6.2. Vision for Next Steps

While we report here the historical progress of the SMM, we are also excited to see where it will go over the next decade. Here we put forward a few of our own personal visions and hopes to try and stimulate future debates, engagement and efforts:

- Data driven approaches: The complexity of real geologic systems is such that uncertainties can be tremendous and these can even be difficult to quantify in 3-d models because of excessive parameters and runtimes. Using analytical or purely theoretical approaches to approximate real systems is an attractive solution but is not necessarily feasible because of their excessive simplicity. This suggests that

finding a parsimonious balance between complex models, theories, and efficient numerical approaches (for data assimilation and model parameterization under uncertainty) might be an excellent way forward, which could build from recent advances in machine and deep learning, as well as other model reduction approaches like polynomial chaos or Gaussian emulation (125; 126). Generally, these are purely numerical approaches, unconstrained by physics, and this can justifiably make users uneasy about actual predictability or extrapolation of information beyond training data sets. However, coupling such methods and constraining them with models based on physical processes, such as the SMM, is an exciting pathway forward to leverage the best of both worlds. This is a place where the simplicity of the SMM is particularly advantageous because it allows one to capture the variability of a complex transport processes using a less complicated model. Reduced complexity numerical approaches could be used to capture the time dependent nature of model parameters (e.g., due to flow variability) or their spatial variability due to the heterogeneity of the subsurface.

- Smart tracers: Most applications of the SMM to date have relied on detailed information that can realistically only be measured in high resolution numerical simulations (e.g. direct measurement of correlation by tracking successive travel times of individual particles). Such methods are not typically possible with current day experimental approaches. However, the advent and continued emergence of novel tracers (e.g. individual particles tagged with unique DNA markers (127; 128)), makes us believe that some day it might actually be possible to obtain such

information in real experiments. While none of the authors of this article are experimentalists, we find the idea of such smart tracers very exciting.

- More seamlessly blending geostatistics with SMMs: As noted above, a major barrier is that most state of the art models require one to run a transport experiment to infer model parameters. Alternative data sources are needed to break this cycle, but the inaccessibility and uncertainty of the subsurface makes it a challenge. One source that is largely overlooked is conceptual geological data, which is typically known with high confidence. We suggest that blending categorical geostatistics, using for example transition probability approaches (25; 15; 129), with SMMs is a natural pairing because both focus on delineating major transitions; changes in geology are strong controls on changes in velocity fields, so there is good reason to expect positive correlation between them. Such a model could be based entirely on commonly available field observables like water levels, borehole tests, well logs, and outcrop analogs, to inform process parameterization in the SMM, which would also provide better connections to data as suggested above. For instance, in the context of heterogeneous conductivity fields' characterization, (23; 130) proposed the link between anomalous transport characteristics and an emerging disorder indicator termed geological entropy. Future works may be directed towards linking such indicators with SMM model parameters.

- Extension to transient flows: Almost all applications of the SMM to porous media flows to date have been under the condition of steady flow conditions (with one notable exception of (91), who considered turbulent flow). Real hydrogeologic systems are rarely, if ever, under true steady state flow conditions as they are continuously forced by intermittent rain events and other elements of the hydrologic cycle, but also by anthropogenic factors like pumping. Extending the SMM to naturally account for temporal variability would require a model framework that relaxes strict stationarity in time, but, considering the linear nature of flow and transport in low Reynolds number settings, it is reasonable to expect that one could do so in a systematic manner that is physically motivated and theoretically based. One approach could be to use stationary (velocity) ranked transition matrices, then scale the velocities up or down as the SMM evolves to account for the impacts of any changes in forcing. This could be as simple as shifting the mean, but in some cases models for the evolution of transition matrices over time might also be needed.

- Generalizing training trajectories: The training trajectory work of (62) is one of the most exciting for us because it is one of the first SMMs that truly attempts to build a model that can predict three-dimensional concentration fields within a still parsimonious framework. Trajectory matching might also be a way of using a combination of synthetic models and data to improve field-scale predictions; however, its current limitation is size. To date, the trajectory-based approach has only been applied in the context of relatively simple sandstone at very small

scales. Trajectory reconstructions are needed for more complex porous media but also at different spatial scales. This could lead to a robust approach for upscaling/predictive purposes where training of the models performed at one scale (sample) could be used to model transport in a different and/or larger sample. This would help develop practical tools for simulating 3-d transport but these will need to be verified against detailed simulations and multi-scale physical experiments to develop confidence.

- Formally connecting Lagrangian and Eulerian view points: For most anomalous transport models that have been used in hydrogeologic systems, one can write clear Eulerian and Lagrangian descriptions of the system (e.g. 32; 41). Typically the Lagrangian picture is written in terms of a discrete equation such as those presented in this paper and the Eulerian one as integro-differential equation (with nonlocal in space and/or time terms). For the SMM, while some efforts have been made, this is not entirely the case. Indeed, we the authors believe that the success of the SMM in periodic systems suggests that one should be able to formally link the Lagrangian framework as we have described it here to the Eulerian framework that evolves from formal upscaling approaches such as volume averaging, where nonlocal in space and time equations can emerge (e.g. 131; 86; 87). Approaches discussed above (93; 114) have shown that numerical closures can be implemented to relate the SMM formulation to subscale features. Establishing a formal link between Eulerian and Lagrangian closures would unlock the possibility to merge the two approaches, which could be beneficial, e.g.

to predict reactive transport processes relying on measurable Eulerian characteristics.

- Connecting state of the art mixing and spreading models: As noted in the previous subsection, the SMM as described here is most conducive to describing one dimensional effective transport, or predicting mean/projected behavior. Another way of expressing this is to say that they do a good job of capturing spreading (i.e. replicating nonlinear scaling of the second centered moment). Nonlinear processes, such as chemical reactions, will require further additions to the SMM. Some exciting developments have taken place in recent years, using the concept of lamellae to describe mixing and reactions in complex heterogeneous systems ranging from pore to Darcy scales (e.g. 132; 133). Elaborating extensively on these would require an entirely new review article, but a large element of these theories relies on balances between mixing and spreading (134). It would be exciting to see the SMM and such approaches coupled together more formally to improve our ability to use the SMM to predict nonlinear processes also.

- Multiphase systems: Multiple fluid phases typically coexist in the subsurface. Examples of common interest of multiphase systems and settings include (i) the unsaturated zone between the Earth's surface and the saturated aquifer where air and water both occupy the void space, (ii) geologic carbon sequestration where supercritical CO2 is injected into saline aquifers for permanent storage so that it cannot access the atmosphere, (iii) conventional and unconventional oil and gas extrac-

tion. Multiphase flows in porous media can be highly complex, leading to even stronger anomalous transport than typically observed. Recent experiments by (135; 136) highlight these very clearly. Another numerical study by (137) highlights that pre-asymptotic anomalous transport at pore scales in a multiphase system can persist for much longer than one would anticipate in a single phase flow. While such observations have been made, applications of the SMM to such systems has been limited. Formally connecting the single phase and multiphase system behaviors within a unified framework with the SMM, perhaps using auto- and cross-transition matrices between the phases, would provide an ability to make more general predictions in real systems of interest.

- Incorporation of further microscale processes from digital rock and soil samples: One of the great advances in porous media over the last decade has been our ability to visualize and measure the full range of complexity at the smallest of scales using innovative technologies able to reconstruct the spatial structure of rock and soil 3D samples and/or and 2D sections (using micro computed tomography, nuclear magnetic resonance, Raman spectroscopy, etc.). To date, these techniques have been used to model the structure of porous media, or the resulting velocity fields, and then impose transport. However, rich data relating to microporosity, mineral composition, heterogeneous reactivity, organic matter/biofilm distributions, imaged phase distributions and so on also exist and all may play a role on how contaminants move and react in real porous media. Being able to incorporate such information in an effective model such as the SMM could be a way to reduce the uncertainty

that currently plagues numerical modeling of biogeochemical processes in soils, e.g. biodegradation of emerging contaminants and agrochemicals (138; 139). New paradigms are needed to incorporate micro-scale information into emerging properties with the aim of constraining predictions, as extensively discussed in a recent review (140). The SMM framework has the potential to overcome the limitation of currently employed approaches, by providing a flexible tool to upscale multi-scale measurements and characterization, going beyond just physical heterogeneity, but embracing the full range of biogeochemical heterogeneity that is ubiquitous in real systems and that can often play an even more important role than previously thought.

Although there are still many obstacles that currently prevent these visions from being realized today, the authors remain optimistic and excited to see the progression of the SMM in the coming years. In just over a decade from conception, significant advances have occurred in SMM research. We expect nothing less than continued growth through the foreseeable future, as field based and computing technologies advance at unprecedented rates. Such technological advancement will expand applications to larger scale geologic systems and other natural flows, while also assisting the scientific community in solving some of the most challenging global problems, including improved methods for energy extraction and mitigating climatic effects induced by anthropogenic emissions. Such advances will also pave the way for new and different models that can hopefully build on the advances presented here. In this review, we have detailed the progression of the SMM and its many successes, while also identifying limitations that must be overcome in order

to bring the SMM (or its successors) to new frontiers.

Acknowledgments

DB and TS were supported by, or in part by, the US Army Research Office under Contract/Grant number W911NF-18-1-0338 as well as by the National Science Foundation under award EAR-1351623. NE was supported by the US Department of Energy, Office of Science under award DE-SC0019123. GP thanks the EU and MIUR for funding, in the frame of the collaborative international Consortium (WE-NEED) financed under the ERA-NET Water-Works2014 Co-funded Call. This ERA-NET is an integral part of the 2015 Joint Activities developed by the Water Challenges for a Changing World Joint Programme Initiative (Water JPI).

References

[1] J. H. Cushman, The physics of fluids in hierarchical porous media: Angstroms to miles, Vol. 10, Springer Science & Business Media, 2013.

[2] G. Dagan, Flow and transport in porous formations, Springer Science & Business Media, 2012.

[3] R. M. Allen-King, I. Kalinovich, D. F. Dominic, G. Wang, R. Polmanteer, D. Divine, Hydrophobic organic contaminant transport property heterogeneity in the borden aquifer, Water Resources Research 51 (3) (2015) 1723–1743.

[4] A. Aubeneau, B. Hanrahan, D. Bolster, J. Tank, Biofilm growth in

gravel bed streams controls solute residence time distributions, Journal of Geophysical Research: Biogeosciences 121 (7) (2016) 1840–1850.

[5] M. M. Meerschaert, Y. Zhang, B. Baeumer, Tempered anomalous diffusion in heterogeneous systems, Geophysical Research Letters 35 (17) (2008) L17403.

[6] M. Dentz, A. Cortis, H. Scher, B. Berkowitz, Time behavior of solute transport in heterogeneous media: transition from anomalous to normal transport, Advances in Water Resources 27 (2) (2004) 155–173.

[7] G. Taylor, Diffusion and mass transport in tubes, Proceedings of the Physical Society. Section B 67 (12) (1954) 857.

[8] R. Aris, On the dispersion of a solute in a fluid flowing through a tube, Proc. R. Soc. Lond. A 235 (1200) (1956) 67–77.

[9] H. Brenner, Macrotransport processes, Elsevier, 2013.

[10] S. Whitaker, The method of volume averaging, Vol. 13, Springer Science & Business Media, 2013.

[11] U. Hornung, Homogenization and porous media, Vol. 6, Springer Science & Business Media, 2012.

[12] J. Auriault, P. Adler, Taylor dispersion in porous media: Analysis by multiple scale expansions, Advances in Water Resources 18 (4) (1995) 217 – 226.

[13] G. De Josselin De Jong, Longitudinal and transverse diffusion in granular deposits, Eos, Transactions American Geophysical Union 39 (1) (1958) 67–74.

[14] P. G. Saffman, A theory of dispersion in a porous medium, Journal of Fluid Mechanics 6 (3) (1959) 321-349.

[15] G. S. Weissmann, S. F. Carle, G. E. Fogg, Three-dimensional hydrofacies modeling based on soil survey analysis and transition probability geostatistics, Water Resources Research 35 (6) (1999) 1761–1770.

[16] S. Y. Lee, S. F. Carle, G. E. Fogg, Geologic heterogeneity and a comparison of two geostatistical models: Sequential Gaussian and transition probability-based geostatistical simulation, Advances in Water Resources 30 (9) (2007) 1914–1932.

[17] N. B. Engdahl, R. M. Maxwell, Quantifying changes in age distributions and the hydrologic balance of a high-mountain watershed from climate induced variations in recharge, Journal of Hydrology 522 (2015) 152–162.

[18] M. Riva, L. Guadagnini, A. Guadagnini, Effects of uncertainty of lithofacies, conductivity and porosity distributions on stochastic interpretations of a field scale tracer test, Stochastic Environmental Research and Risk Assessment 24 (7) (2010) 955–970.

[19] M. Riva, A. Guadagnini, D. Fernandez-Garcia, X. Sanchez-Vila, T. Ptak, Relative importance of geostatistical and transport models

in describing heavily tailed breakthrough curves at the lauswiesen site, Journal of Contaminant Hydrology 101 (1-4) (2008) 1–13.

[20] T. Le Borgne, M. Dentz, J. Carrera, Lagrangian statistical model for transport in highly heterogeneous velocity fields, Physical review letters 101 (9) (2008) 090601.

[21] N. B. Engdahl, T. R. Ginn, G. E. Fogg, Non-Fickian dispersion of groundwater age, Water Resources Research 48 (7) (2012) 1–13.

[22] Y. Edery, A. Guadagnini, H. Scher, B. Berkowitz, Origins of anomalous transport in heterogeneous media: Structural and dynamic controls, Water Resources Research 50 (2) (2014) 1490–1505.

[23] M. Bianchi, D. Pedretti, Geological entropy and solute transport in heterogeneous porous media, Water Resources Research 53 (6) (2017) 4691–4708.

[24] E. Wright, N. Sund, D. Richter, G. Porta, D. Bolster, Upscaling Mixing in Highly Heterogeneous Porous Media via a Spatial Markov Model, Water 11 (1) (2019) 53.

[25] S. F. Carle, G. E. Fogg, Transition probability-based indicator geostatistics, Mathematical Geology 28 (4) (1996) 453–476.

[26] P. Goovaerts, Geostatistics for natural reources evaluation, Oxford University Press, 1997.

[27] G. Dagan, Solute transport in heterogeneous porous formations, Journal of Fluid Mechanics 145 (1984) 151-177.

[28] J. Salles, J.-F. Thovert, R. Delannay, L. Prevors, J.-L. Auriault, P. Adler, Taylor dispersion in porous media. determination of the dispersion tensor, Physics of Fluids A 5 (10) (1992) 2348–2376.

[29] B. Bijeljic, M. J. Blunt, Pore-scale modeling and continuous time random walk analysis of dispersion in porous media, Water resources research 42 (1) (2006) W01202.

[30] R. Haggerty, S. M. Gorelick, Multiple-rate mass transfer for modeling diffusion and surface reactions in media with pore-scale heterogeneity, Water Resources Research 31 (10) (1995) 2383–2400.

[31] D. A. Benson, R. Schumer, M. M. Meerschaert, S. W. Wheatcraft, Fractional dispersion, lévy motion, and the made tracer tests, Transport in porous media 42 (1-2) (2001) 211–240.

[32] B. Berkowitz, A. Cortis, M. Dentz, H. Scher, Modeling non-fickian transport in geological formations as a continuous time random walk, Reviews of Geophysics 44 (2) (2006) RG2003.

[33] A. Cortis, B. Berkowitz, Computing anomalous contaminant transport in porous media: The CTRW Matlab toolbox, Grounwater 43(6) 947-950

[34] J. F. Kelly, D. Bolster, M. M. Meerschaert, J. D. Drummond, A. I. Packman, Fracfit: A robust parameter estimation tool for fractional calculus models, Water Resources Research 53 (3) (2017) 2559–2567.

[35] R. Haggerty, S. M. Wondzell, M. A. Johnson, Power-law residence time

distribution in the hyporheic zone of a 2nd-order mountain stream, Geophysical Research Letters 29 (13) (2002) 18–1.

[36] G. Margolin, M. Dentz, B. Berkowitz, Continuous time random walk and multirate mass transfer modeling of sorption, Chemical physics 295 (1) (2003) 71–80.

[37] S. P. Neuman, D. M. Tartakovsky, Perspective on theories of non-fickian transport in heterogeneous media, Advances in Water Resources 32 (5) (2009) 670–680.

[38] B. Berkowitz, J. Klafter, R. Metzler, H. Scher, Physical pictures of transport in heterogeneous media: Advection-dispersion, random-walk, and fractional derivative formulations, Water Resources Research 38 (10) (2002) 9–1.

[39] R. Schumer, D. A. Benson, M. M. Meerschaert, B. Baeumer, Fractal mobile/immobile solute transport, Water Resources Research 39 (10) (2003) 1296.

[40] M. Dentz, B. Berkowitz, Transport behavior of a passive solute in continuous time random walks and multirate mass transfer, Water Resources Research 39 (5) (2003) 1111.

[41] D. A. Benson, M. M. Meerschaert, A simple and efficient random walk solution of multi-rate mobile/immobile mass transport equations, Advances in Water Resources 32 (4) (2009) 532–539.

[42] B. Noetinger, D. Roubinet, A. Russian, T. Le Borgne, F. Delay,

M. Dentz, J.-R. de Dreuzy, P. Gouze, Random walk methods for modeling hydrodynamic transport in porous and fractured media from pore to reservoir scale, Transport in Porous Media 115 (2) (2016) 345–385.

[43] R. Metzler, J. Klafter, The random walk's guide to anomalous diffusion: a fractional dynamics approach, Physics reports 339 (1) (2000) 1–77.

[44] T. Le Borgne, J.-R. de Dreuzy, P. Davy, O. Bour, Characterization of the velocity field organization in heterogeneous media by conditional correlation, Water resources research 43 (2) (2007) W02419.

[45] S. Painter, V. Cvetkovic, J.-O. Selroos, Power-law velocity distributions in fracture networks: Numerical evidence and implications for tracer transport, Geophysical research letters 29 (14) (2002) 20–1.

[46] S. Painter, V. Cvetkovic, Upscaling discrete fracture network simulations: An alternative to continuum transport models, Water Resources Research 41 (2) (2005) W02002.

[47] S. Painter, V. Cvetkovic, J. Mancillas, O. Pensado, Time domain particle tracking methods for simulating transport with retention and first-order transformation, Water resources research 44 (1) (2008) W01406.

[48] T. Le Borgne, M. Dentz, J. Carrera, Spatial markov processes for modeling lagrangian particle dynamics in heterogeneous porous media, Physical Review E 78 (2) (2008) 026308.

[49] M. Montero, J. Masoliver, Nonindependent continuous-time random walks, Physical Review E 76 (6) (2007) 061115.

[50] V. Tejedor, R. Metzler, Anomalous diffusion in correlated continuous time random walks, Journal of Physics A: Mathematical and Theoretical 43 (8) (2010) 082002.

[51] M. Magdziarz, R. Metzler, W. Szczotka, P. Zebrowski, Correlated continuous-time random walks in external force fields, Physical Review E 85 (5) (2012) 051103.

[52] S. Rogers, C. Van Der Walle, T. Waigh, Microrheology of bacterial biofilms in vitro: Staphylococcus aureus and pseudomonas aeruginosa, Langmuir 24 (23) (2008) 13549–13555.

[53] R. Nathan, W. M. Getz, E. Revilla, M. Holyoak, R. Kadmon, D. Saltz, P. E. Smouse, A movement ecology paradigm for unifying organismal movement research, Proceedings of the National Academy of Sciences 105 (49) (2008) 19052–19059.

[54] C. Song, T. Koren, P. Wang, A.-L. Barabási, Modelling the scaling properties of human mobility, Nature Physics 6 (10) (2010) 818.

[55] E. Scalas, The application of continuous-time random walks in finance and economics, Physica A: Statistical Mechanics and its Applications 362 (2) (2006) 225–239.

[56] M. Montero, J. Masoliver, Continuous time random walks with memory and financial distributions, The European Physical Journal B 90 (11) (2017) 207.

[57] Á. Corral, Dependence of earthquake recurrence times and independence of magnitudes on seismicity history, Tectonophysics 424 (3-4) (2006) 177–193.

[58] P. Manneville, Instabilities, chaos and turbulence, Vol. 1, World Scientific, 2010.

[59] T. Aquino, M. Dentz, A coupled time domain random walk approach for transport in media characterized by broadly-distributed heterogeneity length scales, Advances in water resources 119 (2018) 60–69.

[60] P. K. Kang, M. Dentz, T. Le Borgne, R. Juanes, Spatial markov model of anomalous transport through random lattice networks, Physical review letters 107 (18) (2011) 180602.

[61] P. K. Kang, P. Anna, J. P. Nunes, B. Bijeljic, M. J. Blunt, R. Juanes, Pore-scale intermittent velocity structure underpinning anomalous transport through 3-d porous media, Geophysical Research Letters 41 (17) (2014) 6184–6190.

[62] S. Most, D. Bolster, B. Bijeljic, W. Nowak, Trajectories as training images to simulate advective-diffusive, non-Fickian transport, Water Resources Research 55 (2019) 3465–3480.

[63] T. Le Borgne, D. Bolster, M. Dentz, P. Anna, A. Tartakovsky, Effective pore-scale dispersion upscaling with a correlated continuous time random walk approach, Water Resources Research 47 (12) (2011) W12538.

[64] C. S. Simmons, T. R. Ginn, B. D. Wood, Stochastic-convective transport with nonlinear reaction: Mathematical framework, Water Resources Research 31 (11) (1995) 2675–2688.

[65] T. R. Ginn, E. M. Murphy, A. Chilakapati, U. Seeboonruang, Stochastic-convective transport with nonlinear reaction and mixing: application to intermediate-scale experiments in aerobic biodegradation in saturated porous media, Journal of Contaminant Hydrology 48 (1-2) (2001) 121–149.

[66] A. L. Atchley, R. M. Maxwell, A. K. Navarre-Sitchler, Using streamlines to simulate stochastic reactive transport in heterogeneous aquifers: Kinetic metal release and transport in CO2impacted drinking water aquifers, Advances in Water Resources 52 (2013) 93–106.

[67] N. B. Engdahl, R. M. Maxwell, Approximating groundwater age distributions using simple streamtube models and multiple tracers, Advances in Water Resources 66 (2014) 19–31.

[68] O. A. Cirpka, G. Chiogna, M. Rolle, A. Bellin, Transverse mixing in three-dimensional nonstationary anisotropic heterogeneous porous media, Water Resources Research 51 (2015) 241–260.

[69] G. E. Fogg, C. D. Noyes, S. F. Carle, Geological based model of heterogeneous hydraulic conductivity in an alluvial setting, Hydrogeology Journal 6 (1998) 131–143.

[70] M. M. Meerschaert, M. Dogan, R. L. Van Dam, D. W. Hyndman,

D. A. Benson, Hydraulic conductivity fields: Gaussian or not?, Water Resources Research 49 (2013) 4730–4737.

[71] B. Berkowitz, H. Scher, Anomalous transport in correlated velocity fields, Physical Review E 81 (1) (2010) 011128.

[72] D. Bolster, Y. Méheust, T. Le Borgne, J. Bouquain, P. Davy, Modeling preasymptotic transport in flows with significant inertial and trapping effects–the importance of velocity correlations and a spatial markov model, Advances in water resources 70 (2014) 89–103.

[73] B. Berkowitz, H. Scher, Anomalous transport in random fracture networks, Physical review letters 79 (20) (1997) 4038.

[74] P. K. Kang, T. Le Borgne, M. Dentz, O. Bour, R. Juanes, Impact of velocity correlation and distribution on transport in fractured media: Field evidence and theoretical model, Water Resources Research 51 (2) (2015) 940–959.

[75] P. K. Kang, M. Dentz, R. Juanes, Predictability of anomalous transport on lattice networks with quenched disorder, Physical Review E 83 (3) (2011) 030101.

[76] P. K. Kang, M. Dentz, T. Le Borgne, R. Juanes, Anomalous transport on regular fracture networks: Impact of conductivity heterogeneity and mixing at fracture intersections, Physical Review E 92 (2) (2015) 022148.

[77] P. K. Kang, M. Dentz, T. Le Borgne, S. Lee, R. Juanes, Anomalous transport in disordered fracture networks: Spatial markov model for

dispersion with variable injection modes, Advances in Water Resources 106 (2017) 80–94.

[78] J. D. Hyman, M. Dentz, A. Hagberg, P. K. Kang, Emergence of stable laws for first passage times in three-dimensional random fracture networks, Physical Review Letters 123 (24) (2019) 248501.

[79] J. Hyman, M. Dentz, A. Hagberg, P. K. Kang, Linking structural and transport properties in three-dimensional fracture networks, Journal of Geophysical Research: Solid Earth 124 (2) (2019) 1185–1204.

[80] T. Sherman, J. Hyman, M. Dentz, D. Bolster, Characterizing the influence of fracture density on network scale transport, Journal of Geophysical Research: Solid Earth (2020) e2019JB018547.

[81] A. M. Tartakovsky, S. P. Neuman, Effects of peclet number on pore-scale mixing and channeling of a tracer and on directional advective porosity, Geophysical Research Letters 35 (21) (2008) L21401.

[82] A. M. Tartakovsky, P. Meakin, T. D. Scheibe, R. M. E. West, Simulations of reactive transport and precipitation with smoothed particle hydrodynamics, Journal of Computational Physics 222 (2) (2007) 654–672.

[83] P. De Anna, T. Le Borgne, M. Dentz, A. M. Tartakovsky, D. Bolster, P. Davy, Flow intermittency, dispersion, and correlated continuous time random walks in porous media, Physical review letters 110 (18) (2013) 184502.

[84] R. Friedrich, J. Peinke, M. Sahimi, M. R. R. Tabar, Approaching complexity by stochastic methods: From biological systems to turbulence, Physics Reports 506 (5) (2011) 87–162.

[85] A. Puyguiraud, P. Gouze, M. Dentz, Stochastic dynamics of lagrangian pore-scale velocities in three-dimensional porous media, Water Resources Research 55 (2) (2019) 1196–1217.

[86] Y. Davit, B. D. Wood, G. Debenest, M. Quintard, Correspondence between one-and two-equation models for solute transport in two-region heterogeneous porous media, Transport in porous media 95 (1) (2012) 213–238.

[87] G. Porta, G. Ceriotti, J.-F. Thovert, Comparative assessment of continuum-scale models of bimolecular reactive transport in porous media under pre-asymptotic conditions, Journal of contaminant hydrology 185 (2016) 1–13.

[88] A. Puyguiraud, P. Gouze, M. Dentz, Is there a representative elementary volume for anomalous dispersion?, Transport in Porous Media 131 (2) (2020) 767–778.

[89] B. B. Dykaar, P. K. Kitanidis, Macrotransport of a biologically reacting solute through porous media, Water Resources Research 32 (2) (1996) 307–320.

[90] P. K. Kitanidis, B. B. Dykaar, Stokes flow in a slowly varying two-dimensional periodic pore, Transport in porous media 26 (1) (1997) 89–98.

[91] N. Sund, D. Bolster, S. Mattis, C. Dawson, Pre-asymptotic transport upscaling in inertial and unsteady flows through porous media, Transport in Porous Media 109 (2) (2015) 411–432.

[92] N. L. Sund, D. Bolster, D. A. Benson, Testing the limits of the spatial markov model for upscaling transport: The role of nonmonotonic effective velocity autocorrelations, Physical Review E 94 (4) (2016) 043107.

[93] N. L. Sund, G. M. Porta, D. Bolster, Upscaling of dilution and mixing using a trajectory based spatial markov random walk model in a periodic flow domain, Advances in Water Resources 103 (2017) 76–85.

[94] T. Sherman, A. Fakhari, S. Miller, K. Singha, D. Bolster, Parameterizing the spatial markov model from breakthrough curve data alone, Water Resources Research 53 (12) (2017) 10888–10898.

[95] T. Sherman, A. Foster, D. Bolster, K. Singha, Predicting downstream concentration histories from upstream data in column experiments, Water Resources Research 54 (2018) 9684–9694.

[96] P. K. Kang, S. Brown, R. Juanes, Emergence of anomalous transport in stressed rough fractures, Earth and Planetary Science Letters 454 (2016) 46–54.

[97] P. K. Kang, M. Dentz, T. Le Borgne, S. Lee, R. Juanes, Anomalous transport in disordered fracture networks: spatial markov model for dispersion with variable injection modes, Advances in Water Resources 106 (2017) 80–94.

[98] V. L. Morales, M. Dentz, M. Willmann, M. Holzner, Stochastic dynamics of intermittent pore-scale particle motion in three-dimensional porous media: Experiments and theory, Geophysical Research Letters 44 (18) (2017) 9361–9371.

[99] M. Dentz, P. K. Kang, A. Comolli, T. Le Borgne, D. R. Lester, Continuous time random walks for the evolution of lagrangian velocities, Physical Review Fluids 1 (7) (2016) 074004.

[100] H. Gotovac, V. Cvetkovic, R. Andricevic, Flow and travel time statistics in highly heterogeneous porous media, Water resources research 45 (7) (2009) W07402.

[101] G. Uhlenbeck, L. Ornstein, On the theory of the brownian motion, Physical Review 36 (5) (1930) 823–841.

[102] D. T. Gillespie, Exact numerical simulation of the ornstein-uhlenbeck process and its integral, Physical review E 54 (2) (1996) 2084.

[103] N. G. Van Kampen, Stochastic processes in physics and chemistry, Vol. 1, Elsevier, 1992.

[104] A. Puyguiraud, P. Gouze, M. Dentz, Upscaling of anomalous pore-scale dispersion, Transport in Porous Media 128 (2019) 837–855.

[105] M. Holzner, V. L. Morales, M. Willmann, M. Dentz, Intermittent lagrangian velocities and accelerations in three-dimensional porous medium flow, Physical Review E 92 (1) (2015) 013015.

[106] A. Massoudieh, M. Dentz, J. Alikhani, A spatial markov model for the evolution of the joint distribution of groundwater age, arrival time, and velocity in heterogeneous media, Water Resources Research 53 (7) (2017) 5495–5515.

[107] J. Hyman, M. Dentz, A. Hagberg, P. K. Kang, Linking structural and transport properties in three-dimensional fracture networks, Journal of Geophysical Research: Solid Earth 124 (2019) 1185–1204.

[108] P. K. Kang, Q. Lei, M. Dentz, R. Juanes, Stress-induced anomalous transport in natural fracture networks, Water Resources Research 55 (5) (2019) 4163–4185.

[109] A. Koponen, M. Kataja, J. Timonen, Tortuous flow in porous media, Phys. Rev. E 54 (1996) 406–410.

[110] B. Ghanbarian, A. Hunt, R. Ewing, M. Sahimi, Tortuosity in porous media: A critical review, Soil Science Society of America Journal 77 (5) (2013) 1461–1477.

[111] M. Carrel, V. L. Morales, M. Dentz, N. Derlon, E. Morgenroth, M. Holzner, Pore-scale hydrodynamics in a progressively bioclogged three-dimensional porous medium: 3-d particle tracking experiments and stochastic transport modeling, Water resources research 54 (3) (2018) 2183–2198.

[112] M. Dentz, T. Le Borgne, A. Englert, B. Bijeljic, Mixing, spreading and reaction in heterogeneous media: A brief review, Journal of contaminant hydrology 120 (2011) 1–17.

[113] A. J. Valocchi, D. Bolster, C. J. Werth, Mixing-limited reactions in porous media, Transport in Porous Media 130 (2020) 157–182.

[114] N. Sund, G. Porta, D. Bolster, R. Parashar, A lagrangian transport eulerian reaction spatial (laters) markov model for prediction of effective bimolecular reactive transport, Water Resources Research 53 (11) (2017) 9040–9058.

[115] A. Paster, D. Bolster, D. A. Benson, Connecting the dots: Semi-analytical and random walk numerical solutions of the diffusion–reaction equation with stochastic initial conditions, Journal of Computational Physics 263 (2014) 91–112.

[116] D. Bolster, A. Paster, D. A. Benson, A particle number conserving l agrangian method for mixing-driven reactive transport, Water Resources Research 52 (2) (2016) 1518–1527.

[117] D. A. Benson, D. Bolster, Arbitrarily complex chemical reactions on particles, Water Resources Research 52 (11) (2016) 9190–9200.

[118] N. L. Sund, D. Bolster, C. Dawson, Upscaling transport of a reacting solute through a peridocially converging–diverging channel at preasymptotic times, Journal of contaminant hydrology 182 (2015) 1–15.

[119] T. Sherman, A. Paster, G. Porta, D. Bolster, A spatial markov model for upscaling transport of adsorbing-desorbing solutes, Journal of contaminant hydrology 222 (2019) 31–40.

[120] G. Boccardo, I. M. Sokolov, A. Paster, An improved scheme for a robin

boundary condition in discrete-time random walk algorithms, Journal of Computational Physics 374 (2018) 1152–1165.

[121] T. Sherman, E. B. Janetti, G. R. Guédon, G. Porta, D. Bolster, Upscaling transport of a sorbing solute in disordered non periodic porous domains, Advances in Water Resources (2020) 103574.

[122] S. Most, B. Bijeljic, W. Nowak, Evolution and persistence of cross-directional statistical dependence during finite-péclet transport through a real porous medium, Water Resources Research 52 (11) (2016) 8920–8937.

[123] E. B. Janetti, L. Guadagnini, M. Riva, A. Guadagnini, Global sensitivity analyses of multiple conceptual models with uncertain parameters driving groundwater flow in a regional-scale sedimentary aquifer, Journal of Hydrology 574 (2019) 544–556.

[124] N. Engdahl, D. Bolster, Markovian transport processes in a heterogeneous, variably saturated watershed: A multi-domain spatial markov model, Advances in Water Resources 138 (103555) (2020) 103555.

[125] M. M. Rajabi, Review and comparison of two meta-model-based uncertainty propagation analysis methods in groundwater applications: polynomial chaos expansion and gaussian process emulation, Stochastic Environmental Research and Risk Assessment 33 (2) (2019) 607–631.

[126] N. Fajraoui, F. Ramasomanana, A. Younes, T. Mara, P. Ackerer, A. Guadagnini, Use of global sensitivity analysis and polynomial chaos expansion for interpretation of non-reactive transport experiments

in laboratory-scale porous media, Water Resour. Res. 47(2) (2011) W02521.

[127] H. E. Dahlke, A. G. Williamson, C. Georgakakos, S. Leung, A. N. Sharma, S. W. Lyon, M. T. Walter, Using concurrent dna tracer injections to infer glacial flow pathways, Hydrological Processes 29 (25) (2015) 5257–5274.

[128] C. P. McNew, C. Wang, M. T. Walter, H. E. Dahlke, Fabrication, detection, and analysis of dna-labeled plga particles for environmental transport studies, Journal of colloid and interface science 526 (2018) 207–219.

[129] N. B. Engdahl, G. S. Weissmann, Anisotropic transport rates in heterogeneous porous media, Water Resources Research 46 (2) (2010) 1–12.

[130] M. Bianchi, D. Pedretti, An entrogram-based approach to describe spatial heterogeneity with applications to solute transport in porous media, Water Resources Research 54 (7) (2018) 4432–4448.

[131] B. D. Wood, F. J. Valdes-Parada, Volume averaging: Local and nonlocal closures using a greens function approach, Advances in Water Resources 51 (2013) 139 – 167.

[132] T. Le Borgne, M. Dentz, E. Villermaux, Stretching, coalescence, and mixing in porous media, Physical review letters 110 (20) (2013) 204501.

[133] P. De Anna, M. Dentz, A. Tartakovsky, T. Le Borgne, The filamentary structure of mixing fronts and its control on reaction kinetics in porous media flows, Geophysical Research Letters 41 (13) (2014) 4586–4593.

[134] T. Le Borgne, M. Dentz, P. Davy, D. Bolster, J. Carrera, J.-R. De Dreuzy, O. Bour, Persistence of incomplete mixing: A key to anomalous transport, Physical Review E 84 (1) (2011) 015301.

[135] J. Jiménez-Martínez, P. d. Anna, H. Tabuteau, R. Turuban, T. L. Borgne, Y. Méheust, Pore-scale mechanisms for the enhancement of mixing in unsaturated porous media and implications for chemical reactions, Geophysical Research Letters 42 (13) (2015) 5316–5324.

[136] J. Jiménez-Martínez, T. Le Borgne, H. Tabuteau, Y. Méheust, Impact of saturation on dispersion and mixing in porous media: Photobleaching pulse injection experiments and shear-enhanced mixing model, Water Resources Research 53 (2) (2017) 1457–1472.

[137] D. Triadis, F. Jiang, D. Bolster, Anomalous dispersion in pore-scale simulations of two-phase flow, Transport in Porous Media 126 (2) (2019) 337–353.

[138] J. Greskowiak, E. Hamann, V. Burke, G. Massmann, The uncertainty of biodegradation rate constants of emerging organic compounds in soil and groundwater e A compilation of literature values for 82 substances, Water Research 126 (2017) 122–133.

[139] G. Porta, D. la Cecilia, A. Guadagnini, F. Maggi, Implications of uncertain bioreactive parameters on a complex reaction network of atrazine biodegradation in soil, Advances in Water Resources 121 (2018) 263–276.

[140] P. C. Baveye, W. Otten, A. Kravchenko, M. Balseiro-Romero, E. Beckers, M. Chalhoub, C. Darnault, T. Eickhorst, P. Garnier, S. Hapca, S. Kiranyaz, O. Monga, C. W. Mueller, N. Nunan, V. Pot, S. SchlÃŒter, H. Schmidt, H.-J. Vogel, Emergent properties of microbial activity in heterogeneous soil microenvironments: Different research approaches are slowly converging, yet major challenges remain, Frontiers in Microbiology 9 (2018) 1929.